Atmospheric
Chemistry
and Physics
Discussions

Open Access

Dicarboxylic acids, oxoacids, benzoic acid, α-dicarbonyls, WSOC, OC, and ions in spring aerosols from Okinawa Island in the western North Pacific Rim: size distributions and formation processes

D. K. Deshmukh[1], K. Kawamura[1], M. Lazaar[1,2], B. Kunwar[1], and S. K. R. Boreddy[1]

[1]Institute of Low Temperature Science, Hokkaido University, Sapporo 060-0819, Japan
[2]Ecole National Supérieure de Chimie de Rennes (ENSCR), Rennes 35708, France

Correspondence to: K. Kawamura (kawamura@lowtem.hokudai.ac.jp)

Discussion Paper | Discussion Paper | Discussion Paper | Discussion Paper

ACPD

15, 26509–26554, 2015

Diacids and related compounds in spring aerosols from Okinawa Island

D. K. Deshmukh et al.

Title Page

Abstract	Introduction
Conclusions	References
Tables	Figures

◄ | ►|

◄ | ►

Back | Close

Full Screen / Esc

Printer-friendly Version

Interactive Discussion

Title Page

Abstract | Introduction

Conclusions | References

Tables | Figures

|◄ | ►|

◄ | ►

Back | Close

Full Screen / Esc

Printer-friendly Version

Interactive Discussion

Abstract

Size-segregated aerosols (9-stages from < 0.43 to $> 11.3\,\mu m$ in diameter) were collected at Cape Hedo, Okinawa in spring 2008 and analyzed for water-soluble diacids (C_2–C_{12}), ω-oxoacids (ωC_2–ωC_9), pyruvic acid, benzoic acid and α-dicarbonyls (C_2–C_3) as well as water-soluble organic carbon (WSOC), organic carbon (OC) and major ions. In all the size-segregated aerosols, oxalic acid (C_2) was found as the most abundant species followed by malonic and succinic acids whereas glyoxylic acid (ωC_2) was the dominant oxoacid and glyoxal (Gly) was more abundant than methylglyoxal. Diacids (C_2–C_5), ωC_2 and Gly as well as WSOC and OC peaked at 0.65–1.1 μm in fine mode whereas azelaic (C_9) and 9-oxononanoic (ωC_9) acids peaked at 3.3–4.7 μm in coarse mode. Sulfate and ammonium are enriched in fine mode whereas sodium and chloride are in coarse mode. These results imply that water-soluble species in the marine aerosols could act as cloud condensation nuclei (CCN) to develop the cloud cover over the western North Pacific Rim. The organic species are likely produced by a combination of gas-phase photooxidation, and aerosol-phase or in-cloud processing during long-range transport. The coarse mode peaks of malonic and succinic acids were obtained in the samples with marine air masses, suggesting that they may be associated with the reaction on sea salt particles. Bimodal size distributions of longer-chain diacid (C_9) and oxoacid (ωC_9) with a major peak in the coarse mode suggest their production by photooxidation of biogenic unsaturated fatty acids via heterogeneous reactions on sea salt particles.

1 Introduction

Tropospheric aerosol is an important environmental issue because it can dramatically reduce the visibility (Jacobson et al., 2000; Kanakidou et al., 2005), affect on radiative forcing of climate (Seinfeld and Pandis, 1998), and cause negative impact on human health (Pope and Dockery, 2006). All of these effects strongly depend on the abun-

dances of aerosols and their chemical and physical properties in different sizes. Particles in diameter of 0.1–1.0 µm are very active in scattering and absorbing incoming solar radiation and have a direct impact on climate (Ramanathan et al., 2001; Seinfeld and Pankow, 2003). The knowledge of size distributions of chemical components is thus essential to better understand their potential contributions to climate change and pollution control. Their size distribution also provides evidences for the sources and formation pathways of the atmospheric particles.

The emission sources and multiple secondary formation pathways of organic aerosols are not well understood. Organic compounds account for up to 70 % of fine aerosol mass and potentially control the physicochemical properties of aerosol particles (Davidson et al., 2005; Kanakidou et al., 2005). Low-molecular-weight (LMW) diacids are one of the most abundant organic compound classes in the atmosphere (Kawamura and Ikushima, 1993; Kawamura et al., 1996). They are primarily derived from incomplete combustion of fossil fuel and biomass burning (Kawamura and Kaplan, 1987; Falkovich et al., 2005), and secondarily produced in the atmosphere via photooxidation of unsaturated fatty acids and volatile organic compounds (VOCs) from biogenic and anthropogenic sources (Kawamura and Gagosian, 1987; Kawamura et al., 1996; Sempéré and Kawamura, 2003). The ability of organic aerosols to act as cloud condensation nuclei (CCN) seems to be closely related to their mass-based size distributions (Pradeep Kumar et al., 2003; Ervens et al., 2007).

The increasing atmospheric burden of organic aerosols is associated with natural and anthropogenic emissions in the continental regions. Organic aerosols are eventually transported to the oceanic regions. The rapid industrialization in East Asia is expected to have important influences on global atmospheric chemistry over the next decades (Wang et al., 2013; Tao et al., 2013; Bian et al., 2014). Large amounts of coal burning and biomass burning in East Asia add more anthropogenic aerosols altering the aerosol chemical composition in the remote Pacific atmosphere (Mochida et al., 2007; Miyazaki et al., 2010; Agarwal et al., 2010; Wang et al., 2011; Engling et al., 2013). Water-soluble diacids and related compounds as well as major ions are rarely

Diacids and related compounds in spring aerosols from Okinawa Island

D. K. Deshmukh et al.

studied for their size distributions in remote marine aerosols (Kawamura et al., 2007; Mochida et al., 2007; Miyazaki et al., 2010), whereas their size-segregated characteristics have not been studied in Okinawa Island.

We collected size-segregated aerosol samples with 9-size ranges in spring 2008 in Cape Hedo, Okinawa. Cape Hedo is located on the northern edge of Okinawa Island and can serve as a suitable site for the observation of atmospheric transport of East Asian aerosols with insignificant interference from local emission sources (Takami et al., 2007). The samples were analyzed for dicarboxylic acids (C_2–C_{12}) and related compounds such as ω-oxoacids (ωC_2–ωC_9) and pyruvic acid (C_3) as well as α-dicarbonyls (C_2–C_3) to better understand the sources and processing of water-soluble organic compounds at this marine receptor site in the western North Pacific Rim. Size-segregated samples were also analyzed for water-soluble organic carbon (WSOC), organic carbon (OC), and major inorganic ions. The role of liquid water content of aerosol in the size distribution of diacids and related compounds is discussed. The potential factors responsible for their size distributions and the atmospheric implications of the size characteristics are also discussed.

2 Materials and method

2.1 Site description and aerosol collection

The geographical location of Okinawa Island (26.87° N and 128.25° E) and its surroundings in East Asia are shown in Fig. 1. Okinawa is located in the outflow region of Asian aerosols and on the pathways to the Pacific. Cape Hedo has been used as a supersite of Atmospheric Brown Clouds project to study the atmospheric transport of Chinese aerosols and their chemical transformation during long-range transport from East Asia (Takiguchi et al., 2008; Kunwar and Kawamura, 2014). The sampling site at Cape Hedo is about 60 m a.s.l. Okinawa is a subtropical island (Takiguchi et al., 2008).

Size-segregated aerosol samples were collected at Cape Hedo Atmospheric and Aerosol Monitoring Station (CHAAMS) in 18 March to 13 April 2008. This period is characterized by the westerly wind in the lower troposphere, which is the principal process responsible for the transport of both fossil fuel combustion and biomass burning aerosols in East Asia to the western North Pacific. 9-Stage Andersen Middle Volume Impactor (Tokyo Dylec Company, Japan; $100\,L\,min^{-1}$) was used for the collection of size-segregated samples. The sampler was equipped with 80 mm quartz fiber filters (QFF) that were pre-combusted at $450\,°C$ for 6 h in a furnace to eliminate the adsorbed organic compounds. A total of five sets (OKI-1 to OKI-5) of size-segregated aerosol samples were collected. Each sample set consists of nine filters for the sizes of < 0.43, 0.43–0.65, 0.65–1.1, 1.1–2.1, 2.1–3.3, 3.3–4.7, 4.7–7.0, 7.0–11.3, and $> 11.3\,\mu m$. The filter was placed in a preheated 50 mL glass vial with a Teflon-lined screw cap and stored in a freezer at the station. The samples were stored in darkness at $-20\,°C$ prior to analysis in Sapporo. One set of field blank was collected by placing a pre-combusted QFF for 30 s without sucking air before installing real QFF into the sampler.

2.2 Analytical procedures

Diacids and related compounds were analyzed using the method reported in Kawamura and Ikushima (1993), and Kawamura (1993). Aliquot of the filters were extracted with organic-free ultrapure water (specific resistivity $> 18.2\,M\Omega\text{-cm}$) under ultrasonication. The extracts were passed through glass column packed with quartz wool to remove insoluble particles and filter debris. The extracts were concentrated using a rotary evaporator under vacuum and derivatized to dibutyl esters and dibutoxy acetals with 14 % BF_3 in *n*-butanol at $100\,°C$. Acetonitrile and *n*-hexane were added into the derivatized sample and washed with organic-free pure water. The hexane layer was further concentrated using a rotary evaporator and dried to almost dryness by N_2 blowdown and dissolve in a known volume of *n*-hexane. A 2 µL aliquot of the sample was injected into a capillary GC (Hewlett-Packard HP6890) equipped with an FID detector. Authentic diacid dibutyl esters were used as external standards for the peak identification and

quantification. Identifications of diacids and related compounds were confirmed by GC-mass spectrometry. Recoveries of authentic standards spiked to a pre-combusted QFF were 85 % for oxalic acid (C_2) and more than 90 % for malonic to adipic (C_3–C_6) acids. The analytical errors in duplicate analyses are within 10 % for major species.

To measure water-soluble organic carbon (WSOC), a punch of 20 mm diameter of each QFF was extracted with organic-free ultrapure water in a 50 mL glass vial with a Teflon-lined screw cap under ultrasonication for 15 min. The water extracts were subsequently passed through a syringe filter (Millex-GV, Millipore; diameter of 0.22 μm). The extract was first acidified with 1.2 M HCl and purged with pure air in order to remove dissolve inorganic carbon and then WSOC was measured using a total organic carbon (TOC) analyzer (Shimadzu TOC-V$_{CSH}$) (Miyazaki et al., 2011). External calibration was performed using potassium hydrogen phthalate before analysis of WSOC. The sample was measured three times and the average value was used for the calculation of WSOC concentrations. The analytical error in the triplicate analysis was 5 % with a detection limit of 0.1 μg C m^{-3}.

Organic and elemental carbon (OC and EC) was determined using a Sunset Lab carbon analyzer following the Interagency Monitoring of Protected Visual Environments (IMPROVE) thermal evolution protocol as described in detail by Wang et al. (2005a). Presence of carbonate carbon in the aerosol samples was assumed to be negligible. A filter disc of 1.5 cm^2 was placed in a quartz tube inside the thermal desorption chamber of the analyzer and then stepwise heating was applied. Helium (He) gas is applied in the first ramp and is switched to mixture of He/O$_2$ in the second ramp. The evolved CO$_2$ during the oxidation at each temperature step was measured with non-dispersive infrared (NDIR) detector system. The analytical errors in the triplicate analysis of the filter sample were estimated to be 5 % for OC and EC. EC was detected only in fine fractions. The concentration of total carbon (TC) was calculated by summing the concentrations of OC and EC in each size fraction.

For the determination of major ions, a punch of 20 mm diameter of each filter was extracted with organic-free ultrapure water under ultrasonication. These extracts were

filtered through a disc filter (Millex-GV, Millipore; diameter of 0.22 µm) and injected to ion chromatograph (Compact IC 761; Metrohm, Switzerland) for measuring MSA^-, Cl^-, SO_4^{2-}, NO_3^-, Na^+, NH_4^+, K^+, Ca^{2+}, and Mg^{2+} (Boreddy and Kawamura, 2015). Anions were separated on a SI-90 4E Shodex column (Showa Denko; Tokyo, Japan) using a mixture of 1.8 mM Na_2CO_3 and 1.7 mM $NaHCO_3$ solution at a flow rate of 1.2 mL min^{-1} as an eluent and 40 mM H_2SO_4 for a suppressor. A Metrosep C2-150 Metrohm column was used for cation analysis using a mixture of 4 mM tartaric acid and 1 mM dipicolinic acid solution as an eluent at a flow rate of 1.0 mL min^{-1}. The injected loop volume was 200 µL. The detection limits for anions and cations were ca. 0.1 ng m^{-3}. The analytical error in duplicate analysis was about 10 %. The concentrations of all diacids and inorganic ions reported here are corrected for field blanks.

2.3   Backward air mass trajectories

The air mass backward trajectory was computed for the sampling period using the Hybrid Single-Particle Lagrangian Integrated Trajectory (HYSPLIT) model 4.0 developed by the National Oceanic and Atmospheric Administration (NOAA) Air Resources Laboratory (ARL) (Draxler and Rolph, 2013). The seven-day trajectories at 500 m above the ground level for the samples collected in Okinawa are shown in Fig. 2. Okinawa was strongly affected by continental air masses from Siberia and Mongolia as well as North China and Korea. It is difficult to differentiate the source regions of air masses for each sample set because the sampling duration for each sample was 3–5 days. Each sample contains mixed continental and oceanic air masses.

2.4   Estimation of liquid water content (LWC) of aerosol

Liquid water content (LWC) of aerosol was calculated for the size-segregated samples collected in Okinawa Island using the ISORROPIA II model (Fountoukis and Nenes, 2007). ISORROPIA II is a computationally efficient and rigorous thermodynamic equilibrium model that exhibits robust and rapid convergence under all aerosol types with

Title Page

Abstract | Introduction

Conclusions | References

Tables | Figures

|◄ | ►|

◄ | ►

Back | Close

Full Screen / Esc

Printer-friendly Version

Interactive Discussion

high computational speed (Nenes et al., 1998). Measured concentrations of water-soluble inorganic ions were used for the estimation of aerosol LWC.

3   Results and discussion

3.1   Size-segregated aerosol chemical characteristics

We use 2.1 µm as a split diameter between the fine and coarse mode particles because there is no cut size of 2.5 µm in the air sampler used in this study. Table 1 presents the concentrations of inorganic and carbonaceous species in the fine and coarse mode aerosols. Figure 3 shows the average concentrations of inorganic ions and organic matter (OM) in size-segregated aerosols. Abundances of OM in the atmosphere are generally estimated by multiplying the measured OC mass concentrations with the conversion factor of 1.6 for urban aerosols and 2.1 for aged aerosols (Turpin and Lim, 2001). Our sampling site Cape Hedo is located in the outflow region of East Asian aerosols and local anthropogenic activities are insignificant. Because Okinawa aerosols are subjected to aging processes to result in more oxygenated organic species during long-range transport (Takami et al., 2007; Takiguchi et al., 2008; Kunwar and Kawamura, 2014), we use the conversion factor of 2.1 instead of 1.6 to calculate OM for the Okinawa samples.

Sulfate was the most abundant anion in fine fractions whereas chloride was the dominant anion in coarse fractions. The cation budget was largely controlled by ammonium in fine mode whereas sodium was identified as the most abundant cation in coarse mode. The high abundance of SO_4^{2-} in fine particles suggests a significant contribution of anthropogenic sources including industrial emissions in East Asia via long-range transport of aerosols over the western North Pacific Rim. The abundant presence of NH_4^+ together with SO_4^{2-} in the same fraction demonstrated that ammonium sulfate is the major form of sulfate in the Okinawa aerosols. SO_4^{2-} is an anthropogenic tracer of industrial activities whereas NH_4^+ is the secondary product of NH_3 that is largely de-

rived from the agricultural usage of nitrogen-based fertilizers (Pakkanen et al., 2001) and volatilization from soils and livestock waste in East Asia (Huang et al., 2006). The dominant presences of Na^+ and Cl^- in coarse fractions suggest an important contribution from sea salt. Na^+ and Cl^- are emitted from the ocean surface as relatively larger particles. Very small amount of NO_3^- was detected in Okinawa aerosols, suggesting a formation of $NaNO_3$ or $Ca(NO_3)_2$ in coarse fractions through the reaction of gaseous HNO_3 onto pre-existing alkaline particles.

Diacids and related compounds detected in Okinawa are listed in Table 2 together with their concentrations in the fine and coarse modes. Their molecular distributions in size-segregated aerosols are shown in Fig. 4. Oxalic acid (C_2) was found as the most abundant diacid followed by malonic (C_3) and succinic (C_4) acids in all size-segregated aerosols. The predominance of C_2 on the fine mode suggested that this diacid is produced by the photooxidation of VOCs and other organic precursors in gas and aqueous-phase (Warneck, 2003; Carlton et al., 2006) during long-range transport. The abundant presence of C_3 also indicates that this diacid was produced from atmospheric photooxidation of C_4 diacid during long-range transport to Okinawa (Kawamura and Sakaguchi, 1999; Kunwar and Kawamura, 2014).

Phthalic (Ph) and adipic (C_6) acids are the next abundant diacids whereas ketomalonic acid (kC_3) is more abundant than C_6 diacid in the size ranges of 0.43–0.65 to 0.65–1.1 μm. The predominance of kC_3 after Ph in fine fractions indicates an enhanced photochemical oxidation process of organic aerosols during long-range transport. Although Ph is directly emitted from combustion sources (Kawamura and Kaplan, 1987), the secondary formation via photooxidation of aromatic hydrocarbons such as gaseous naphthalene (NAP) may be more significant in the Okinawa aerosols during long-range transport. High NAP levels were reported in gas and aerosols from East Asia (Liu et al., 2007; Tao et al., 2007), further supporting NAP as a potential precursor of Ph in Okinawa aerosols. Kawamura and Usukura (1993) reported that C_6 diacid is an oxidation product through the reaction of cyclohexene with ozone (O_3).

Diacids and related compounds in spring aerosols from Okinawa Island

D. K. Deshmukh et al.

Title Page

Abstract	Introduction
Conclusions	References
Tables	Figures

|◄ | ►|

◄ | ►

Back | Close

Full Screen / Esc

Printer-friendly Version

Interactive Discussion

Azelaic acid (C_9) is always more abundant than the adjacent suberic (C_8) and decanedioic (C_{10}) acids in all the size-segregated aerosols. Kawamura and Gagosian (1987) proposed that C_9 is produced by photooxidation of unsaturated fatty acids such as oleic acid ($C_{18:1}$) containing a double bond at C-9 position. Unsaturated fatty acids can be emitted from sea surface microlayers and from local vegetation in Okinawa (Kunwar and Kawamura, 2014). Moreover, air masses in spring are suggested to originate mostly from Russia and Mongolia as well as Korea based on seven-day backward trajectory analyses. The abundant presence of C_9 diacid indicates a significant atmospheric processing of aerosols during long-range transport via ozonolysis or OH-initiated oxidation of unsaturated fatty acids derived from phytoplankton or terrestrial higher plants. ω-Oxocarboxylic acids and α-dicarbonyls were also detected in the Okinawa aerosols. Glyoxylic acid (ωC_2) was identified as the most abundant ω-oxoacid whereas glyoxal (Gly) was more abundant than methylglyoxal in all the sizes. The predominance of ωC_2 and Gly indicates that they are key precursors of C_2 diacid in Okinawa aerosols.

3.2 Inorganic species

The particle size distributions of major ions are shown in Fig. 5. Pearson correlation coefficients (r) among the measured ions in different size modes of five set samples are given in Table 3. It is clear that Na^+ and Cl^- are mainly derived from the ocean surface as sea salt (Kumar et al., 2008; Geng et al., 2009). The size distributions of Na^+ and Cl^- were found to be unimodal with a peak at $> 11.3\,\mu m$ in most sample sets (OKI-1 and OKI-3 to OKI-5) (Fig. 5a and b). Their peaks at $> 11.3\,\mu m$ suggest that they are of marine origin due to bubble bursting of surface seawater. We also found the second peak of Na^+ and Cl^- at 2.1–3.3 or 3.3–4.7 μm. Andreas (1998) suggested that the sea spray fall into two types that are defined as film and jet bubbles; film bubbles correspond to the smaller size of 0.5–5 μm whereas jet bubbles produce the larger size of 5–20 μm. The coarse mode peaks at 2.1–3.3 μm or 3.3–4.7 as well as $> 11.3\,\mu m$ in Okinawa aerosols are associated with film and jet bubbles. The accumulation of these

species in smaller sizes may be caused by anthropogenic emissions such as waste incineration in East Asia and secondary aerosol formation during long-range transport (Yao et al., 2002). We found that size distribution of Mg^{2+} is similar to those of Na^+ and Cl^- in $> 11.3\,\mu m$ with a significant positive correlation to coarse mode Na^+ and Cl^- ($r = 0.98$), suggesting their similar origin and sources.

A significant contribution of Ca^{2+} in coarse mode particles demonstrates its contributions from soil dust (Kerminen et al., 1997; Tsai and Chen, 2006). A lifting of soil dust in continental sites followed by subsequent long-range atmospheric transport to remote marine site is also proposed as an important source of Ca^{2+} (Wang et al., 2005b). Ca^{2+} showed unimodal distribution with a peak at either 2.1–3.3 or 3.3–4.7 μm (Fig. 5c). The coarse mode Ca^{2+} is mostly derived from crustal $CaCO_3$, which heterogeneously reacts with acidic gases (HNO_3 and SO_2) (Kerminen et al., 1997). This formation mechanism is further supported by a strong correlation of coarse mode Ca^{2+} with NO_3^- ($r = 0.98$). There is no correlation between Ca^{2+} and Na^+ or Cl^- (-0.12 or -0.27), revealing that sea salt contribution of Ca^{2+} is negligible in Okinawa aerosols. This result suggests that the long-range transport of soil dust is an important contributor of Ca^{2+} in the marine aerosols from the western North Pacific Rim. Backward trajectories also indicated that the air masses originated from Siberia and Mongolia are transported to Okinawa. Such air mass origin again indicates a long-range transport of Asian dust from East Asia to the western North Pacific.

Potassium is enriched in biomass burning aerosols and therefore its abundances in fine particles can serve as a diagnostic tracer of biomass burning (Yamasoe et al., 2000). Moreover, contributions of K^+ from sea salt and dust sources are highly variable in regional case studies with its dominance in coarse mode particles. Fresh biomass burning particles mostly reside in the condensation mode at 0.1–0.5 μm in diameter whereas the fine mode K^+ of biomass burning origin can be subjected to in-cloud processing (Kaufman and Fraser, 1997; Kleeman and Cass, 1999), in which K^+ can act as effective CCN together with abundant water-soluble organic compounds. The size distribution of K^+ is characterized by bimodal pattern with peaks at 0.65–1.1 and 2.1–

3.3 μm in OKI-1 sample set (Fig. 5e) whereas another set of sample (OKI-5) showed a peak at 4.7–7.0 μm followed by 0.65–1.1 μm in diameter. A unimodal size distribution of K^+ was observed in other three sets of samples with a peak at 0.65–1.1 μm in the fine mode.

5   The peak of K^+ at 0.65–1.1 μm suggests a contribution from biomass burning aerosols (Falkovich et al., 2005; Huang et al., 2006). The fine mode nss-K^+ accounted for 95 % of the total K^+ in the OKI-2 sample set and 88 % of that in the OKI-3 sample set when air masses are coming from Siberia and Mongolia as well as North China. The abundant presence of fine mode nss-K^+ in the OKI-2 and OKI-3 samples further
10 indicates the long-range atmospheric transport of biomass burning aerosols from the Asian continent to the western North Pacific Rim. The coarse mode K^+ was strongly correlated with the coarse mode Cl^- ($r = 0.90$). This result suggests that the coarse mode K^+ in the sample sets OKI-1 and OKI-5 may be derived from sea salt particles. The coarse mode K^+ can also originate from coagulation of small biomass burning
15 particles onto large particles.

    NO_x is known to be a precursor of NO_3^-, which can be converted to HNO_3 and then react with NH_3 to form NH_4NO_3. A unimodal size distribution of NO_3^- was observed with a peak at 2.1–3.3 or 3.3–4.7 μm in diameter. It should also be noted that the NO_3^- concentration in the coarse mode is much higher than that in the fine mode (Table 1). This
20 result suggests that either dust or sea salt particle is the source of coarse mode NO_3^- in Okinawa. Coarse mode NO_3^- is the product of heterogeneous reaction of gaseous NO_2 or HNO_3 with alkaline metals such as Na^+ and Ca^{2+} as shown in Reactions (R1) and (R2) (Kouyoumdjian and Saliba, 2006; Seinfeld and Pandis, 2006).

$$HNO_{3(g)} + NaCl_{(aq\,and\,s)} \rightarrow NaNO_{3(aq\,and\,s)} + HCl_{(g)} \qquad (R1)$$
25 $$2HNO_{3(g)} + CaCO_{3(s)} \rightarrow Ca(NO_3)_{2(s)} + H_2O + CO_{2(g)} \qquad (R2)$$
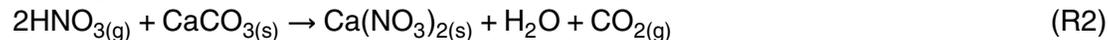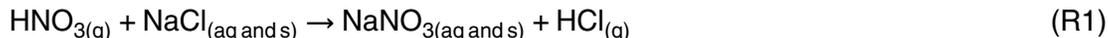
As discussed earlier, the air masses originated from Siberia are transported over Mongolia and North China. Asian dust can be transported from the Asian continent to Okinawa. Therefore, it is possible that the gaseous HNO_3 might already have reacted with

CaCO$_3$ (mineral dust particle) to from NO$_3^-$ before arriving to Okinawa through Reaction (R2). We found that coarse mode Na$^+$, which is derived from sea salts, is negatively correlated ($r = -0.30$) with the coarse mode NO$_3^-$, suggesting an insignificant production of NO$_3^-$ on the coarse mode through Reaction (R1) in Okinawa aerosols. NO$_3^-$

5 peaked at the same particle size of Ca^{2+}. Therefore, NO$_3^-$ in Okinawa coarse mode aerosols is probably resulted from the pickup of HNO$_3$ gas by soil dust particles enriched with Ca^{2+} via heterogeneous reaction near the source regions. This process is further supported by a good correlation between NO$_3^-$ and Ca^{2+} (0.98) in the coarse mode.

10 The particle size distributions of SO$_4^{2-}$, which is the major source of acid deposition (Pakkanen et al., 2001), have been the subject of numerous studies in the past few decades (Huang et al., 2006; Kouyoumdjian and Saliba, 2006). Condensation mode SO$_4^{2-}$ arises from gas-phase oxidation of SO$_2$ followed by gas-to-particle conversion whereas fine mode SO$_4^{2-}$ is formed through aqueous-phase oxidation of SO$_2$ in clouds.

15 SO$_4^{2-}$ on the coarse mode can be attributed to a combination of sulfate and heterogeneous reactions of SO$_2$ on soil dust or sea salt particles (Seinfeld and Pandis, 1998; Pakkanen et al., 2001). A unimodal size distribution of SO$_4^{2-}$ was observed with a peak at 0.65–1.1 µm. This result suggests that SO$_4^{2-}$ is produced from in-cloud aqueous oxidation of SO$_2$ with OH radical and O$_3$.

20 LWC can influence the aqueous oxidation of SO$_2$ with OH radical and O$_3$ in the fine mode. Calculated LWC for each sample from Okinawa and average LWC in size-segregated aerosols are shown in Fig. 6. The most remarkable result of the calculation is the different LWC among the particles of different sizes. We clearly found two peaks of LWC in fine and coarse modes. The difference in LWC in size-segregated aerosols is

25 undoubtedly due to the difference in their chemical composition. We observed that the highest LWC was found at the size of 0.65–1.1 µm in the fine mode in Okinawa samples. The high LWC at 0.65–1.1 µm size fractions should enhance the uptake of more SO$_2$ and accelerate its photooxidation in aerosol aqueous phase to form new sulfate

Diacids and related compounds in spring aerosols from Okinawa Island

D. K. Deshmukh et al.

Title Page

Abstract	Introduction
Conclusions	References
Tables	Figures

|◄ | ►|

◄ | ►

Back | Close

Full Screen / Esc

Printer-friendly Version

Interactive Discussion

particles during long-range atmospheric transport in East Asia. It is further supported by the significant positive correlation between LWC and SO_4^{2-} ($r = 0.92$) in fine mode.

Methanesulfonate (MSA), which is produced by gas-to-particle conversion via the oxidation of dimethyl sulfide (DMS) emitted from the ocean (Quinn et al., 1993), shows size distribution similar to SO_4^{2-}, indicating that oxidation of DMS also contribute to the formation of SO_4^{2-} during long-range transport. This size distribution of MSA observed over Okinawa is consistent with previous studies from the China Sea by Gao et al. (1996), who suggested that MSA is produced through the oxidation of S-containing species in the marine atmosphere.

NH_4^+ in the Okinawa aerosols shows a unimodal size distribution with a peak at 0.65–1.1 µm (Fig. 5h), indicating that NH_4^+ is mainly formed by gas-to-particle conversion via the reaction with H_2SO_4 and possibly organic acids. Interestingly, the size distributions of NH_4^+ were similar to those of SO_4^{2-} and diacids such as oxalic acid (C_2) (Figs. 5g and 8a). This result implies that the formation of NH_4^+ in the fine mode is affected by the presence of SO_4^{2-} and C_2 diacid. We found a strong correlation between SO_4^{2-} and NH_4^+ on the fine mode ($r = 0.99$). This good correlation suggests that NH_4^+ is present as ammonium sulfate in aerosols. We found that NH_4^+ showed a good correlation ($r = 0.87$) with LWC in the fine mode. This result implies that the abundant presence of SO_4^{2-} and NH_4^+ in fine mode enhanced the LWC in fine mode of Okinawa aerosols. It is notable that higher LWC in fine mode can influence the SOA formation via gas to particle conversion of organic precursors and subsequent heterogeneous reactions in aqueous phase.

Kerminen et al. (1997) proposed that particulate NH_4^+ is secondarily formed via heterogeneous reactions of gaseous NH_3 with acidic species such as sulfur dioxide and sulfuric acid. NH_4^+ exists mainly in fine fractions in the form of $(NH_4)_2SO_4$ and NH_4HSO_4 in the atmosphere. We also found a good correlation between NH_4^+ and oxalic acid ($r = 0.89$) in fine mode although the correlation is poor ($r = 0.26$) in coarse mode. The occurrence of ammonium oxalate may be important in fine fraction of Okinawa aerosols. This implication is further supported by Boreddy et al. (2014), who found

that NH_4^+ was highly correlated with C_2 diacid in $PM_{2.5}$ fraction of Tanzanian biomass burning aerosols.

3.3   Water-soluble organic carbon (WSOC) and organic carbon (OC)

The size distributions of water-soluble organic carbon (WSOC) and organic carbon (OC) for five sample sets at Okinawa are shown in Fig. 7. Their concentrations in the fine and coarse mode aerosols are summarized in Table 1. As stated before, elemental carbon (EC) was detected only in fine size bins (Table 1).

The mass-based size distribution of WSOC is characterized by a major peak at 0.65–1.1 µm in fine mode and by a small peak at 3.3–4.7 µm in coarse mode. Huang et al. (2006) observed that fine mode WSOC is derived from secondary photochemical sources and primary combustion products. It is well recognized that biofuel combustion and biomass burning produce a large amount of WSOC (Mayol-Bracero et al., 2002). The WSOC concentrations showed a statistically significant correlation with fine mode SO_4^{2-} ($r = 0.96$). Because production of SO_4^{2-} is strongly linked to photochemical activity, this result suggests an important secondary production of WSOC in fine mode particles during long-range atmospheric transport from East Asia. The WSOC concentrations also showed high correlation with K^+ ($r = 0.93$) and NH_4^+ (0.91) in the fine mode. This result suggests that both biomass burning and photochemical production contribute significantly to the formation of fine mode WSOC in Okinawa aerosols during long-range transport.

Fine mode WSOC concentrations in OKI-1 to OKI-4 aerosol samples are 3–5 times higher (1.09 µg m^{-3} for OKI-4 to 1.61 µg m^{-3} for OKI-2) than that in the sample OKI-5 (0.31 µg m^{-3}). It is also noteworthy that fine mode fraction of WSOC in the samples OKI-1 to OKI-4 contributed 70–75 % of total WSOC. We noted that the former 4 sample sets are more influenced by continental air masses than the last set (Fig. 2). These results suggested that WSOC is more enriched in the samples with an influence of continental air masses from Siberia and Mongolia as well as North China and Korea. Because WSOC is an important fraction of OC in Okinawa aerosols, high loadings of

WSOC in aerosols of continental air masses suggest that both fossil fuel combustion and biomass burning in East Asia may have a significant impact on air quality and chemical and physical properties of aerosols, causing possible changes in the climate over the western North Pacific.

The mass-size distribution pattern of OC is similar to that of WSOC with a major peak in the size range of 0.65–1.1 µm whereas a small peak was appeared in the larger size range of 3.3–4.7 µm in diameter. The major fine mode peak of OC may be resulted from in-cloud processing of organic aerosols during long-range atmospheric transport from East Asia. The significant positive correlations of fine mode OC with K^+ ($r = 0.95$) and secondary inorganic species such as SO_4^{2-} ($r = 0.93$) and NH_4^+ (0.91) further support the contribution of cloud-processed biomass burning products to fine mode OC in Okinawa aerosols.

A significant portion of OC may be oxidized to WSOC during the atmospheric transport from East Asia to the western North Pacific. The mass ratio of WSOC/OC has been proposed as a measure of photochemical processing or aging of organics especially in long-range transported aerosols (Aggarwal and Kawamura, 2009). The WSOC/OC ratios varied from 0.51–0.76 with an average of 0.67 ± 0.09 in the fine mode and 0.43–0.63 with an average of 0.55 ± 0.09 in the coarse mode. The higher WSOC/OC ratio in fine mode suggests that organics are more significantly subjected to photochemical processing in fine mode aerosols during long-range transport from the Asian continent to Okinawa than coarse mode aerosols.

It is noteworthy that ratio of WSOC/OC and LWC significantly correlates in the fine mode with $r = 0.87$. The significant positive correlation in the fine mode samples further suggests that enhancement of LWC in fine aerosols is favorable for aqueous phase photooxidation of OC to WSOC in Okinawa samples. This result may also indicate that shorter-chain organic compounds with polar functional group such as diacids and oxoacids as well as α-dicarbonyls may contribute more to fine mode WSOC via oxidation of various organic precursors in gas and aqueous-phase during long-range transport (Carlton et al., 2007; Miyazaki et al., 2010). Kawamura et al. (2005, 2007)

proposed that shorter-chain diacids and related polar compounds are significantly produced via photochemical oxidation of various precursors and thus they are abundantly present in fine particles contributing more to WSOC fraction.

3.4 Dicarboxylic acids

The size distributions of selected diacids and related compounds are shown in Fig. 8. Oxalic acid (C_2) showed a peak at 0.65–1.1 μm in fine mode (Fig. 8a). This result suggests that size distribution of C_2 diacid was not significantly influenced by dust or sea salt particles that may cause a shift of the peak from fine to coarse mode in the size distributions (Kerminen et al., 1999; Mochida et al., 2003a). The shift of smaller diacids (C_2–C_4) from submicron to supermicron mode has been observed in marine aerosols collected from the western North Pacific in spring when a strong outflow of Asian dusts occurred. Mochida et al. (2003a, 2007) reported that a supermicron peak of diacids was emerged by the uptake of gaseous diacids on sea salt particles based on the similarity between sea salt surface area and diacids size distributions or heterogeneous oxidations of organic precursors on the sea salt particles.

The fine mode peak of C_2 in Okinawa aerosols suggests that this diacid is produced by photochemical oxidation of gaseous precursors during long-range atmospheric transport. We found that size distribution of C_2 diacid is similar to that of SO_4^{2-} (Figs. 5g and 8a), suggesting a similar formation pathway probably via in-cloud processing. A good correlation between C_2 and SO_4^{2-} ($r = 0.92$) in fine mode further supports that C_2 is a secondary photochemical product. C_2 diacid also showed a significant positive correlation with fine mode K^+ ($r = 0.85$), which is a tracer of biomass burning particles that are active as effective CCN in the atmosphere. A good correlation between fine mode C_2 and SO_4^{2-} or K^+ indicates that photochemical production and biomass burning both contributed significantly to C_2 diacid at 0.65–1.1 μm in fine mode.

Several sources are known to oxalic acid (C_2) in atmospheric aerosols. They include primary sources and secondary formation via photooxidation of anthropogenic and bio-

Title Page

Abstract | Introduction

Conclusions | References

Tables | Figures

◄ | ►

◄ | ►

Back | Close

Full Screen / Esc

Printer-friendly Version

Interactive Discussion

genic precursors (Kawamura and Sakaguchi, 1999). C_2 is produced by the photooxidation of malonic acid (C_3) (Kawamura and Ikushima, 1993). C_2 and C_3 are formed by the photooxidation of succinic acid (C_4) whereas C_4 is produced by the photooxidation of glutaric acid (C_5) (Kawamura and Ikushima, 1993). The fine mode predominance of C_2 in Okinawa aerosols was probably associated with an enhanced aqueous oxidation of anthropogenic precursors emitted in East Asia during long-range transport. Lim et al. (2005) and Legrand et al. (2007) reported the formation of diacids in aqueous phase. Here we investigate the impact of LWC of aerosols on the formation of diacids in Okinawa aerosols. Higher LWC can enhance the partitioning of the gaseous organic precursors into the aerosol aqueous phase for the formation of C_2 diacid. We found that the fine mode peak of C_2 is consistent with that of LWC in Okinawa samples (Figs. 6b and 8a). A strong positive correlation ($r = 0.92$) of C_2 with LWC in fine mode confirms that enhanced LWC in fine mode is favorable for the aqueous phase production of C_2 from its precursor compounds in Okinawa aerosols.

The robust correlations of C_2 with C_3–C_5 diacids ($r = 0.89$–0.92) indicate the production of C_2 diacid via decay of longer-chain diacids during long-range transport. This result is further supported by the good correlations of C_3–C_5 diacids with LWC ($r = 0.82$–0.89) in the fine mode. Another pathway for the production of C_2 diacid is the aqueous oxidation of glyoxylic acid (ωC_2) produced by the photooxidation of glyoxal (Gly) and methylglyoxal (MeGly) (Lim et al., 2005). Gly and MeGly are easily hydrated and partitioned into the aerosol phase with lifetime less than 3 h (Kampf et al., 2012). Fine mode C_2 showed a significant positive correlation with ωC_2 ($r = 0.99$) and Gly (0.93) whereas weak correlation was found with MeGly (0.62). These results suggest that ωC_2 and Gly are important precursors of C_2 diacid and increased LWC in fine mode is favorable for aqueous phase oxidation of ωC_2 and Gly to result in C_2.

Malonic acid (C_3) peaked at 0.65–1.1 μm in diameter (Fig. 8b), being similar to C_2 diacid (Fig. 8a), except for two sets of samples (OKI-1 and OKI-5) that showed peaks at 2.1–3.3 or 3.3–4.7 μm in the coarse mode. Succinic acid (C_4) showed two peaks at the size bins of 0.65–1.1 and 2.1–3.3 μm in OKI-1 whereas in OKI-5 sample set C_4

Diacids and related compounds in spring aerosols from Okinawa Island

D. K. Deshmukh et al.

Title Page

Abstract	Introduction
Conclusions	References
Tables	Figures

|◄ | ►|

◄ | ►

Back | Close

Full Screen / Esc

Printer-friendly Version

Interactive Discussion

showed additional peak at $> 11.3\,\mu m$ (Fig. 8c). The coarse mode peaks of this diacid in samples OKI-1 and OKI-5 may be associated with sea salt particles because the samples have an influence of marine air masses during the sampling period.

Kawamura and Ikushima (1993) proposed that the ratio of malonic to succinic acid (C_3/C_4) is a tracer to indicate the extent of photochemical processing of longer chain diacids such as glutaric acid (C_5). Because C_4 is oxidized to C_3, an increase in the C_3/C_4 ratio indicates an increased processing, assuming that C_3 does not have an additional source and that C_4 does not have an additional sink in aqueous phase. The averaged C_3/C_4 ratio in sum of all the size fractions was found to be 1.5 ± 0.1 in Okinawa aerosols. This result suggests that the extent of photochemical processing is much greater in Okinawa than Los Angeles (0.35) (Kawamura and Kaplan, 1987) but similar to that of urban Tokyo (1.5) (Kawamura and Ikushima, 1993), whereas it is lower than those of marine aerosols at Chichijima Island in the western North Pacific (2.0) (Mochida et al., 2003b) and the remote Pacific including tropics (3.9) (Kawamura and Sakaguchi, 1999). Figure 9a shows changes in the C_3/C_4 ratios as a function of particle size. The C_3/C_4 ratios exhibit higher values at 1.1–$2.1\,\mu m$ in fine mode and at 2.1–3.3 and 3.3–$4.7\,\mu m$ in coarse mode. This result suggests that C_3 production via C_4 decomposition occurs more efficiently at these size ranges by aqueous-phase processing.

It is noteworthy that emission sources can also control the size distributions of organic compounds. A bimodal size distribution of C_9 diacid was observed in Okinawa aerosols with a major peak on coarse mode at 3.3–$4.7\,\mu m$ and minor peak on fine mode at 0.65–$1.1\,\mu m$ (Fig. 8f). Kawamura and Gagosian (1987) reported that photooxidation of unsaturated fatty acids such as oleic ($C_{18:1}$) and linoleic ($C_{18:2}$) acids produces azelaic acid (C_9) in the marine atmosphere. These fatty acids can be emitted from sea surface microlayers. The major peak of C_9 diacid on coarse mode suggests that photooxidation of phytoplankton-derived unsaturated fatty acids from the ocean with sea salt particles is an important source in Okinawa aerosols (Mochida et al., 2007; Agarwal et al., 2010). Unsaturated fatty acids can also be directly emitted as fine particles

from combustion sources such as biomass burning and food cooking in East Asia and long-range transported to the western North Pacific (Agarwal et al., 2010; Wang et al., 2012). The minor peak of C_9 in fine mode can be explained by the oxidation of fine-mode unsaturated fatty acids derived from biomass burning or gaseous unsaturated
5 fatty acids.

A unimodal size distribution was obtained for phthalic acid (Ph) with a fine mode peak at 0.65–1.1 µm, except for one sample set (OKI-5) that showed a bimodal distribution with almost equal peaks at 0.65–1.1 and 2.1–3.3 µm (Fig. 8g). This aromatic diacid is a tracer of anthropogenic sources and significantly produced by the photooxidation
10 of anthropogenic precursors such as naphthalene emitted from incomplete combustion of fossil fuel (Kawamura and Kaplan, 1987). The major peak of Ph on fine mode can be explained by the gas-phase photooxidation of naphthalene and its subsequent condensation on pre-existing fine particles during long-range atmospheric transport. The comparable coarse mode peak in the OKI-5 sample set suggests an adsorption
15 of gaseous Ph onto larger particles. Terephthalic acid (tPh), which is a tracer of plastic burning (Kawamura and Pavuluri, 2011), showed a unimodal distribution peaking at the size bin of 0.65–1.1 µm (Fig. 8h). tPh is mostly emitted from the burning of plastic wastes such as plastic bags and bottles, and then deposited on pre-existing fine particles.

20 Phthalic acid (Ph) is mostly derived by photochemical oxidation of aromatic hydrocarbons emitted from automobiles and fossil fuel combustion whereas azelaic acid (C_9) has been proposed as a secondary oxidation product of biogenic unsaturated fatty acids containing a double bond at C-9 position (Kawamura and Ikushima, 1993; Kawamura and Gagosian, 1987). The Ph/C_9 ratios can provide relative contributions
25 of anthropogenic and biogenic sources. Figure 9b shows the changes in the ratios of Ph/C_9 as a function of particle sizes. The higher Ph/C_9 ratios were obtained on the fine mode particles than coarse mode particles. The results suggest that fine aerosols are significantly influenced by anthropogenic sources whereas the coarse aerosols are more influenced by biogenic sources. The significant contribution of Ph on the fine

Diacids and related compounds in spring aerosols from Okinawa Island

D. K. Deshmukh et al.

Title Page

Abstract	Introduction
Conclusions	References
Tables	Figures

|◄ | ►|

◄ | ►

Back | Close

Full Screen / Esc

Printer-friendly Version

Interactive Discussion

mode demonstrates that this aromatic diacid is mainly produced by the photooxidation of aromatic hydrocarbons such as naphthalene emitted from fossil fuel combustion in gas phase followed by condensation of the product onto pre-existing fine particles during long-range transport in the atmosphere.

3.5 ω-Oxocarboxylic acids and pyruvic acid

ω-Oxocarboxylic acids (ωC_2–ωC_9) are secondarily produced in the atmosphere and also directly emitted from fossil fuel combustion and biomass burning. They are further oxidized into diacids via the oxidation of aldehyde group of the compounds (Kawamura et al., 1996; Warneck, 2003). The size distribution of glyoxylic acid (ωC_2) shows a unimodal pattern with a peak at 0.65–1.1 µm (Fig. 8i). A bimodal size distribution of 4-oxobutanoic acid (ωC_4) was observed with two peaks at 0.65–1.1 and 2.1–3.3 µm in the first set of sample (OKI-1), which is comparable to those of the size distribution of C_4 diacid in the same sample set. ωC_4 in other sample sets (OKI-2 to OKI-5) showed unimodal size distribution with a peak at 0.65–1.1 µm. The small peak of ωC_4 in coarse mode at 2.1–3.3 µm may be associated with heterogeneous oxidation of unsaturated fatty acids on sea salt particles.

Mochida et al. (2007) reported a strong bimodal pattern of oxoacids with a peak in the coarse aerosol mode off the coast of East Asia. They suggested that the larger mode was likely due to either uptake of oxoacids or their heterogeneous reactions on sea salt particles. Soil dust or sea salt particles may also affect the size distribution of semi-volatile oxoacids in Okinawa aerosols because both particles were clearly observed at diameters greater than 2.1 µm (Fig. 5a–c). The fine mode maxima of oxoacids indicate that they are secondarily produced in the atmosphere by the photochemical oxidation of gaseous precursors during long-range transport to Okinawa. Interestingly, we found that size distribution of C_2 diacid is similar to that of ωC_2 oxoacid (Fig. 8a and i). Furthermore, similar size distributions were observed for C_4 diacid and ωC_4 oxoacid (Fig. 8c and j). Those similarities suggest that both diacids and ω-oxoacids are simultaneously produced via gas and aqueous-phase oxidation of their precursors.

The diacids may be produced by the oxidation of corresponding ω-oxoacids in aerosols during long-range transport.

The important precursor of ωC_2 in atmospheric aerosols is Gly and MeGly (Lim et al., 2005; Myriokefalitakis et al., 2011). We found that ωC_2 is strongly correlated with Gly ($r = 0.92$) and moderately correlated with MeGly (0.55) in the fine mode. The former result suggests that Gly is a key precursor of ωC_2 in Okinawa aerosols. The significant positive correlation of ωC_2 with LWC (0.95) in fine mode further suggests that an increase in LWC enhanced the aqueous phase oxidation of Gly to produce ωC_2 in fine mode. The strong correlation of fine mode ωC_2 with SO_4^{2-} (0.96) further confirms secondary formation of ωC_2 from the precursors originated from anthropogenic and biogenic sources during long-range transport to Okinawa. Although the enhanced ωC_2 concentrations in fine mode might be a result of aqueous oxidation, ωC_2 may be rather controlled by biomass burning activity. This is supported by the significant positive correlation of ωC_2 with K^+ ($r = 0.90$) in the fine mode.

A bimodal size distribution was observed for 9-oxononanoic acid (ωC_9) (Fig. 8k). We found that the peak at 3.3–4.7 µm in coarse mode is larger than that at 0.65–1.1 µm in fine mode. Again, size distribution of ωC_9 is similar to that of C_9 diacid. ωC_9 is another counterpart of photooxidation product of biogenic unsaturated fatty acids such as oleic ($C_{18:1}$) acid having a double bond at C-9 position (Kawamura and Gagosian, 1987). Although air masses during the sampling period are mostly originated from Siberia, Mongolia, Korea and North China (Fig. 2), where unsaturated fatty acids of higher plant origin are abundantly supplied to this marine receptor site, sea surface microlayers and local vegetation in Okinawa can also emit unsaturated fatty acids abundantly. Therefore, the major peak of ωC_9 on the coarse mode may indicate that photochemical oxidation of unsaturated fatty acids of oceanic phytoplankton origin via heterogeneous reaction on sea salt particles is more important than those of terrestrial higher plant origin (Mochida et al., 2007; Agarwal et al., 2010).

Pyruvic acid (Pyr) showed a bimodal size distribution with a major peak on coarse mode at the size of 3.3–4.7 or 7.0–11.3 µm and a minor peak on fine mode at the

Title Page

Abstract | Introduction

Conclusions | References

Tables | Figures

|◄ | ►|

◄ | ►

Back | Close

Full Screen / Esc

Printer-friendly Version

Interactive Discussion

size of 0.65–1.1 µm. The larger peak of Pyr on coarse mode may suggest that pyruvic acid is possibly produced by the heterogeneous photooxidation of isoprene emitted from the ocean surface probably on sea salt particles. Several studies suggested that Pyr is produced via the aqueous-phase photooxidation of methylglyoxal (MeGly) that is a gas-phase oxidation product of isoprene emitted from the ocean surface (Lim et al., 2005; Carlton et al., 2006).

3.6 α-Dicarbonyls

Glyoxal (Gly) and methylglyoxal (MeGly) are gas-phase oxidation products of numerous VOCs such as benzene, toluene and xylene (Volkamer et al., 2001) as well as ethylene and isoprene (Zimmermann and Poppe, 1996) and terpenes (Lim et al., 2005). Gly may be associated with pollution sources whereas MeGly may be involved with biogenic sources. Gly peaked at 0.65–1.1 µm in the fine mode in the Okinawa samples. The fine mode peak of Gly is similar to those of K^+ and SO_4^{2-} (Fig. 5e and g), suggesting their similar sources and formation pathways in the aerosols. Although gas-phase oxidation of isoprene has been reported as the largest global source of Gly (Zimmermann and Poppe, 1996), oxidation of anthropogenic aromatic hydrocarbons from fossil fuel combustion and biomass burning is also suggested as alternative source of Gly in the atmosphere (Jung et al., 2010). The peak of Gly at 0.65–1.1 µm may be associated with the combustion sources and the subsequent gas-phase oxidation of the precursors during long-range transport to Okinawa. A good correlation of Gly with K^+ or NH_4^+ ($r = 0.86$) in fine mode further suggests that biomass burning is a major source of fine mode Gly in Okinawa aerosols.

In contrast, we found a bimodal size distribution of MeGly with two peaks on the fine and coarse modes. Biogenic VOCs such as isoprene emitted from the ocean surface are subjected to oxidation leading to the formation of MeGly in the atmosphere through aqueous-phase chemistry (Carlton et al., 2006; Ervens et al., 2008). The peak of MeGly on coarse mode suggests that MeGly might be produced by the aqueous-phase oxidation of isoprene emitted from the ocean surface on sea salt particles. MeGly could

Title Page

Abstract | Introduction

Conclusions | References

Tables | Figures

|◀ | ▶|

◀ | ▶

Back | Close

Full Screen / Esc

Printer-friendly Version

Interactive Discussion

act as a precursor of secondary organic aerosols (SOA) in the atmosphere (Kroll et al., 2005; Liggio et al., 2005). Gly and MeGly are largely present in gaseous phase and only small portion is in ambient aerosols (Kawamura et al., 2013), although hydrated Gly and MeGly likely exist in aerosols. However, aerosol phase α-dicarbonyls are important in terms of heterogeneous oxidation to result in oxalic acid, which is the most abundant organic species in aerosols. The oxidation of α-dicarbonyls in aerosol phase should promote their transfer from gas to particle phase, affecting the gas/aerosol partitioning of Gly and MeGly, which may have a significant effect on the chemical and physical properties of aerosols and thus radiating forcing of atmospheric particles.

3.7 Benzoic acid

The size distribution of benzoic acid is presented in Fig. 8o. Two sample sets (OKI-1 and OKI-2) showed unimodal size distribution of benzoic acid with a peak at 0.65–1.1 or 1.1–2.1 µm in the fine mode. Benzoic acid is directly emitted from the automobile emissions (Kawamura et al., 1985) and secondarily produced by photochemical oxidation of automobile-derived aromatic compounds (Ho et al., 2006). Although benzoic acid is semi-volatile and mainly found in gas-phase (Kawamura et al., 2000; Fraser et al., 1998), it can be observed in particulate phase via gas-to-particle conversion by forming salts such as ammonium benzoate or potassium benzoate. Duan et al. (2008) reported high level of ambient toluene (11 µg m^{-3}) in China during an ozone episode in 2006 and suggested that photooxidation of toluene is one of major sources of benzoic acid in the atmosphere.

The major peak of benzoic acid at small size bin of 0.65–1.1 or 1.1–2.1 µm suggest that a significant portion of this compound in the Okinawa aerosols is likely produced by gas-to-particle conversion via the reaction with NH$_3$ and alkaline metals and the subsequent deposition onto pre-existing fine particles during long-range transport. We observed an additional small peak of benzoic acid at 4.7–7.0 µm on the coarse mode for the sample sets of OKI-3 to OKI-5. Because benzoic acid mainly exists in gas-phase in the atmosphere due to the relatively high volatility (Fraser et al., 1998), the

Title Page

Abstract | Introduction

Conclusions | References

Tables | Figures

◀ | ▶|

◀ | ▶

Back | Close

Full Screen / Esc

Printer-friendly Version

Interactive Discussion

small peak on the coarse mode indicates a potential adsorption of gaseous benzoic acid onto larger particles that may contain alkaline Na, K and Ca, or uptake by sea spray water droplets emitted from sea surface.

4 Summary and conclusions

Nine-stage aerosol particles from < 0.43 to $> 11.3\,\mu m$ in diameter, collected in spring 2008 at Cape Hedo, Okinawa in the western North Pacific Rim, were analyzed for water-soluble diacids and related compounds as well as major ions. The molecular distributions of diacids were characterized by the predominance of oxalic acid (C_2) followed by malonic and succinic acids in all stages, suggesting that they are most likely produced by the photooxidation of VOCs and particulate organic precursors in the source region and/or during long-range atmospheric transport. The abundant presence of SO_4^{2-} as well as phthalic and adipic acids in Okinawa suggested the significant contributions of anthropogenic sources including industrial emissions in East Asia via long-range atmospheric transport.

SO_4^{2-}, NH_4^+, and diacids up to 5-carbon atoms as well as glyoxylic acid (ωC_2) and glyoxal (Gly) showed good correlations with peaks in fine mode (0.65–1.1 μm). WSOC and OC also peaked on fine mode with an additional minor peak on coarse mode. An important mechanism for the formation of these species in Okinawa aerosols is probably gas-phase oxidation of VOCs and the subsequent in-cloud processing during long-range atmospheric transport. The strong correlations of fine mode SO_4^{2-} and NH_4^+ with LWC imply that abundant presences of SO_4^{2-} and NH_4^+ in fine mode promote to enhance the LWC in fine mode of Okinawa aerosols, which is favorable for the aqueous oxidation of precursor compounds to result in C_2 (r is 0.91 for LWC and C_2). The robust correlations of C_2 with C_3–C_5 diacids as well as ωC_2 and Gly indicate that they are the key precursors of C_2 diacid in Okinawa aerosols. Their characteristic size distribution implies that particles enriched with these species could act as CCN, enhancing the cloud cover over the western North Pacific Rim.

We observed an enrichment of malonic and succinic acids on coarse mode particles in the aerosols with marine air mass origin, indicating that their formation is associated with the heterogeneous reactions on sea salt particles. Longer-chain diacid (C_9) and ω-oxoacid (ωC_9) showed bimodal size distribution with a major peak on coarse mode, suggesting that they are produced by photooxidation of unsaturated fatty acids mainly derived from phytoplankton via heterogeneous reactions on sea spray particles. We observed that WSOC and OC in fine particles are photochemically more processed in the atmosphere than in coarse particles during long-range transport. This study demonstrates that anthropogenic and biomass burning aerosols emitted from East Asia have significant influence on the molecular compositions of water-soluble organic aerosols in the western North Pacific Rim.

References

Agarwal, S., Aggarwal, S. G., Okuzawa, K., and Kawamura, K.: Size distributions of dicarboxylic acids, ketoacids, α-dicarbonyls, sugars, WSOC, OC, EC and inorganic ions in atmospheric particles over Northern Japan: implication for long-range transport of Siberian biomass burning and East Asian polluted aerosols, Atmos. Chem. Phys., 10, 5839–5858, doi:10.5194/acp-10-5839-2010, 2010.

Aggarwal, S. G. and Kawamura, K.: Carbonaceous and inorganic composition in long-range transported aerosols over northern Japan: implicationsn for aging of water-soluble organic fraction, Atmos. Environ., 43, 2532–2540, 2009.

Andreas, E. L.: A new sea spray generation function for wind speeds up to $32\,m\,s^{-1}$, J. Phys. Oceanogr., 28, 2175–2184, 1998.

Bian, Q., Huang, X. H. H., and Yu, J. Z.: One-year observations of size distribution characteristics of major aerosol constituents at a coastal receptor site in Hong Kong – Part 1: Inorganic ions and oxalate, Atmos. Chem. Phys., 14, 9013–9027, doi:10.5194/acp-14-9013-2014, 2014.

Boreddy, S. K. R. and Kawamura, K.: A 12 year observation of water-soluble ions in TSP aerosols collected at a remote marine location in the western North Pacific: an outflow region of Asian dust, Atmos. Chem. Phys., 15, 6437–6453, doi:10.5194/acp-15-6437-2015, 2015.

Boreddy, S. K. R., Kimitaka, K., Mkoma, S., and Fu, P.: Hygroscopic behavior of water-soluble matter extracted from biomass burning aerosols collected at a rural site in Tanzania, East Africa, J. Geophys. Res., 105, 4501–4512, 2014.

Carlton, A. G., Turpin, B. J., Lim, H. J., Altieri, K. E., and Seitzinger, S.: Link between isoprene and secondary organic aerosol (SOA): pyruvic acid oxidation yields low volatility organic acids in clouds, Geophys. Res. Lett., 33, L06822, doi:10.1029/2005GL025374, 2006.

Carlton, A. G., Turpin, B. J., Altieri, K. E., Seitzinger, S., Reff, A., Lim, H. J., and Ervens, B.: Atmospheric oxalic acid and SOA production from glyoxal: results of aqueous photooxidation experiments, Atmos. Environ., 41, 7588–7602, 2007.

Corrigan, A. L., Johnson, A. M., Song, W., Keronen, P., Königstedt, R., Williams, J., Russell, L. M., Petäjä, T., Fischer, H., and Hoffmann, T.: First measurements of reactive α-dicarbonyl concentrations on $PM_{2.5}$ aerosol over the Boreal forest in Finland during HUMPPA-COPEC 2010 – source apportionment and links to aerosol aging, Atmos. Chem. Phys., 12, 6145–6155, doi:10.5194/acp-12-6145-2012, 2012.

Davidson, C. I., Phalen, R. F., and Solomon, P. A.: Airborne particulate matter and human health: a review, Aerosol. Sci. Tech., 39, 737–749, 2005.

Draxler, R. R. and Rolph, G. D.: HYSPLIT (HYbrid Single-Particle Lagrangian Integrated Trajectory) Model, available at: http://www.arl.noaa.gov/HYSPLI~T.php (last access: 5 January 2015), NOAA Air Resouces Laboratory, College Park, MD, 2013.

Duan, J. C., Tan, J. H., Yang, L., Wu, S., and Hao, J. M.: Concentration, sources and ozone formation potential of volatile organic compounds (VOCs) during ozone episode in Beijing, Atmos. Res., 88, 25–35, 2008.

Engling, G., Lee, J. J., Sie, H. J., Wu, Y. C., and Yet-Pole, I.: Anhydrosugar characteristics in biomass smoke aerosol-case study of environmental influence on particle-size of rice straw burning aerosol, J. Aerosol Sci., 56, 2–14, 2013.

Ervens, B., Cubison, M., Andrews, E., Feingold, G., Ogren, J. A., Jimenez, J. L., DeCarlo, P., and Nenes, A.: Prediction of cloud condensation nucleus number concentration using measurements of aerosol size distributions and composition and light scattering enhancement due to humidity, J. Geophys. Res., 112, D10S32, doi:10.1029/2006jd007426, 2007.

Ervens, B., Carlton, A. G., Turpin, B. J., Altieri, K. E., Kreidenweis, S. M., and Feingold, G.: Secondary organic aerosol yields from cloud-processing of isoprene oxidation products, Geophys. Res. Lett., 35, L02816, doi:10.1029/2007gl031828, 2008.

Falkovich, A. H., Graber, E. R., Schkolnik, G., Rudich, Y., Maenhaut, W., and Artaxo, P.: Low molecular weight organic acids in aerosol particles from Rondonia, Brazil, during the biomass-burning, transition and wet periods, Atmos. Chem. Phys., 5, 781–797, doi:10.5194/acp-5-781-2005, 2005.

Fountoukis, C. and Nenes, A.: ISORROPIA II: a computationally efficient thermodynamic equilibrium model for K^+–Ca^{2+}–Mg^{2+}–NH_4^+–Na^+–SO_4^{2-}–NO_3^-–Cl^-–H_2O aerosols, Atmos. Chem. Phys., 7, 4639–4659, doi:10.5194/acp-7-4639-2007, 2007.

Fraser, M. P., Cass, G. R., and Simoneit, B. R. T.: Gas-phase and particle-phase organic compounds emitted from motor vehicle traffic in a Los Angeles roadway tunnel, Environ. Sci. Technol., 32, 2051–2060, 1998.

Gao, Y., Arimoto, R., Duce, R. A., Chen, L. Q., Zhou, M. Y., and Gu, D. Y.: Atmospheric non-sea-salt sulfate, nitrate and methanesulfonate over the China Sea, J. Geophys. Res., 101, 12601–12611, 1996.

Geng, H., Park, Y., Hwang, H., Kang, S., and Ro, C.-U.: Elevated nitrogen-containing particles observed in Asian dust aerosol samples collected at the marine boundary layer of the Bohai Sea and the Yellow Sea, Atmos. Chem. Phys., 9, 6933–6947, doi:10.5194/acp-9-6933-2009, 2009.

Ho, K. F., Lee, S. C., Cao, J. J., Kawamura, K., Watanabe, T., Cheng, Y., and Chow, J. C.: Dicarboxylic acids, ketocarboxylic acids and dicarbonyls in the urban roadside area of Hong Kong, Atmos. Environ., 40, 3030–3040, 2006.

Huang, X. F., Yu, J. Z., He, L. Y., and Yuan, Z. B.: Water-soluble organic carbon and oxalate in aerosols at a coastal urban site in China: size distribution characteristics, sources, and formation mechanisms, J. Geophys. Res., 111, D22212, doi:10.1029/2006JD007408, 2006.

Jacobson, M. C., Hansson, H. C., Noone, K. J., and Charlson, R. J.: Organic atmospheric aerosols: review and state of science, Rev. Geophys., 38, 267–294, 2000.

Jung, J. S., Tsatsral, B., Kim, Y. J., and Kawamura, K.: Organic and inorganic aerosol compositions in Ulaanbaatar, Mongolia, during the cold winter of 2007 to 2008: Dicarboxylic acids, ketocarboxylic acids, and alpha-dicarbonyls, J. Geophys. Res., 115, D22203, doi:10.1029/2010JD014339, 2010.

Kampf, C. J., Corrigan, A. L., Johnson, A. M., Song, W., Keronen, P., Konigstedt, R., Williams, J., Russel, L. M., Petaja, T., Fischer, H., and Hoffmann, T.: First measurement of reactive alpha-dicarbonyl concentrations on $PM_{2.5}$ aerosols over the Boreal forest in Finland during HUMPPA-COPEC 2010 – source apportionment and links to aerosol aging, Atmos. Chem. Phys., 12, 6145–6155, doi:10.5194/acp-12-6145-2012, 2012.

Kanakidou, M., Seinfeld, J. H., Pandis, S. N., Barnes, I., Dentener, F. J., Facchini, M. C., Van Dingenen, R., Ervens, B., Nenes, A., Nielsen, C. J., Swietlicki, E., Putaud, J. P., Balkanski, Y., Fuzzi, S., Horth, J., Moortgat, G. K., Winterhalter, R., Myhre, C. E. L., Tsigaridis, K., Vignati, E., Stephanou, E. G., and Wilson, J.: Organic aerosol and global climate modelling: a review, Atmos. Chem. Phys., 5, 1053–1123, doi:10.5194/acp-5-1053-2005, 2005.

Kaufman, Y. J. and Fraser, R. S.: The effect of smoke particles on clouds and climate forcing, Science, 277, 1636–1639, 1997.

Kawamura, K.: Identification of C_2–C_{10} ω-oxocarboxylic acids, pyruvic acid, and C_2–C_3 α-dicarbonyls in wet precipitation and aerosol samples by capillary GC and GC/MS, Anal. Chem., 65, 3505–3511, 1993.

Kawamura, K. and Gagosian, R. B.: Implications of ω-oxocarboxylic acids in the remote marine atmosphere for photo-oxidation of unsaturated fatty acids, Nature, 325, 330–332, 1987.

Kawamura, K. and Ikushima, K.: Seasonal changes in the distribution of dicarboxylic acids in the urban atmosphere, Environ. Sci. Technol., 27, 2227–2235, 1993.

Kawamura, K. and Kaplan, I. R.: Motor exhaust emissions as a primary source for dicarboxylic-acids in Los-Angeles ambient air, Environ. Sci. Technol., 21, 105–110, 1987.

Kawamura, K. and Pavuluri, C. M.: New directions: need for better understanding of plastic waste burning as inferred from high abundance of terephthalic acid in South Asian aerosols, Atmos. Environ., 44, 5320–5321, 2011.

Diacids and related compounds in spring aerosols from Okinawa Island

D. K. Deshmukh et al.

Title Page

Abstract | Introduction

Conclusions | References

Tables | Figures

◄ | ►

◄ | ►

Back | Close

Full Screen / Esc

Printer-friendly Version

Interactive Discussion

Kawamura, K. and Sakaguchi, F.: Molecular distributions of water soluble dicarboxylic acids in marine aerosols over the Pacific Ocean including tropics, J. Geophys. Res., 104, 3501–3509, 1999.

Kawamura, K. and Usukura, K.: Distributions of low molecular weight dicarboxylic acids in the North Pacific aerosol samples, J. Oceanogr., 49, 271–283, 1993.

Kawamura, K., Ng, L., and Kaplan, I. R., Determination of organic acids (C_1–C_{10}) in the atmosphere, motor-exhausts and engine oils, Environ. Sci. Technol., 19, 1082–1086, 1985.

Kawamura, K., Kasukabe, H., and Barrie, L. A.: Source and reaction pathways of dicarboxylic acids, ketoacids and dicarbonyls in arctic aerosols: one year of observations, Atmos. Environ., 30, 1709–1722, 1996.

Kawamura, K., Steinberg, S., and Kaplan, I. R.: Homologous series of C_1–C_{10} monocarboxylic acids and C_1–C_6 carbonyls in Los Angeles air and motor vehicle exhausts, Atmos. Environ., 34, 4175–4191, 2000.

Kawamura, K., Imai, Y., and Barrie, L. A.: Photochemical production and loss of organic acids in high Arctic aerosols during long-range transport and polar sunrise ozone depletion events, Atmos. Environ., 39, 599–614, 2005.

Kawamura, K., Narukawa, M., Li, S. M., and Barrie, L. A.: Size distributions of dicarboxylic acids and inorganic ions in atmospheric aerosols collected during polar sunrise in the Canadian high Arctic, J. Geophys. Res., 112, D10307, doi:10.1029/2006JD008244, 2007.

Kawamura, K., Okuzawa, K., Aggarwal, S. G., Irie, H., Kanaya, Y., and Wang, Z.: Determination of gaseous and particulate carbonyls (glycolaldehyde, hydroxyacetone, glyoxal, methylglyoxal, nonanal and decanal) in the atmosphere at Mt. Tai, Atmos. Chem. Phys., 13, 5369–5380, doi:10.5194/acp-13-5369-2013, 2013.

Kerminen, V. M., Pakkanen, T. A., and Hillamo, R. E.: Interactions between inorganic trace gases and supermicrometer particles at a coastal site, Atmos. Environ., 31, 2753–2765, 1997.

Kerminen, V. M., Teinila, K., Hillamo, R., and Makela, T.: Size-segregated chemistry of particulate dicarboxylic acids in the Arctic atmosphere, Atmos. Environ., 33, 2089–2100, 1999.

Kleeman, M. J. and Cass, G. R.: Effect of emissions control strategies on the size and composition distribution of urban particulate air pollution, Environ. Sci. Technol., 33, 177–189, 1999.

Kouyoumdjian, H. and Saliba, N. A.: Mass concentration and ion composition of coarse and fine particles in an urban area in Beirut: effect of calcium carbonate on the absorption of

nitric and sulfuric acids and the depletion of chloride, Atmos. Chem. Phys., 6, 1865–1877, doi:10.5194/acp-6-1865-2006, 2006.

Kroll, J. H., Ng, N. L., Murphy, S. M., Varutbangkul, V., Flagan, R. C., and Seinfeld, J. H.: Chamber studies of secondary organic aerosol growth by reactive uptake of simple carbonyl compounds, J. Geophys. Res., 110, D23207, doi:10.1029/2005jd006004, 2005.

Kumar, A., Sarin, M. M., and Sudheer, A. K.: Mineral and anthropogenic aerosols in Arabian Sea-atmospheric boundary layer: sources and spatial variability, Atmos. Environ., 42, 5169–5181, 2008.

Kunwar, B. and Kawamura, K.: Seasonal distribution and sources of low molecular weight dicarboxylic acids, ω-oxocarboxylic acids, pyruvic acid, α-dicarbonyls and fatty acids in ambient aerosols from subtropical Okinawa in the western Pacific Rim, Environ. Chem., 11, 673–689, 2014.

Legrand, M., Preunkert, S., Oliveira, T., Pio, C. A., Hammer, S., Gelencser, A., Kasper-Giebl, A., and Laj, P.: Origin of C_2-C_5 dicarboxylic acids in the European atmosphere inferred from year-round aerosol study conducted at a west–east transect, J. Geophys. Res., 112, D23S07, doi:10.1029/2006JD008019, 2007.

Liggio, J. L., Li, S. M., and McLaren, R.: Reactive uptake of glyoxal by particulate matter, J. Geophys. Res., 110, D10304, doi:10.1029/2004JD005113, 2005.

Lim, H. J., Carlton, A. G., and Turpin, B. J.: Isoprene forms secondary organic aerosol through cloud processing: model simulations, Environ. Sci. Technol., 39, 4441–4446, 2005.

Liu, S. Z., Tao, S., Liu, W. X., Liu, Y. N., Dou, H., Zhao, J. Y., Wang, L. G., Wang, J. F., Tian, Z. F., and Gao, Y.: Atmospheric polycyclic aromatic hydrocarbons in north China: a winter-time study, Environ. Sci. Technol., 41, 8256–8261, 2007.

Mayol-Bracero, O. L., Guyon, P., Graham, B., Roberts, G., Andreae, M. O., Decesari, S., Facchini, M. C., Fuzzi, S., and Artaxo, P.: Water-soluble organic compounds in biomass burning aerosols over Amazonia – 2. Apportionment of the chemical composition and importance of the polyacidic fraction, J. Geophys. Res., 107, 8091, doi:10.1029/2001jd000522, 2002.

Miyazaki, Y., Kawamura, K., and Sawano, M.: Size distributions and chemical characterization of water-soluble organic aerosols over the western North Pacific in summer, J. Geophys. Res., 115, D23210, doi:10.1029/2010JD014439, 2010.

Miyazaki, Y., Kawamura, K., Jung, J., Furutani, H., and Uematsu, M.: Latitudinal distributions of organic nitrogen and organic carbon in marine aerosols over the western North Pacific, Atmos. Chem. Phys., 11, 3037–3049, doi:10.5194/acp-11-3037-2011, 2011.

Title Page

Abstract | Introduction

Conclusions | References

Tables | Figures

◄ | ►►

◄ | ►

Back | Close

Full Screen / Esc

Printer-friendly Version

Interactive Discussion

Mochida, M., Kawamura, K., Umemoto, N., Kobayashi, M., Matsunaga, S., Lim, H. J., Turpin, B. J., Bates, T. S., and Simoneit, B. R. T.: Spatial distributions of oxygenated organic compounds (dicarboxylic acids, fatty acids, and levoglucosan) in marine aerosols over the western Pacific and off the coast of East Asia: continental outflow of organic aerosols during the ACE-Asia campaign, J. Geophys. Res., 108, 8638, doi:10.1029/2002JD003249, 2003a.

Mochida, M., Umemoto, N., Kawamura, K., and Uematsu, M.: Bimodal size distribution of C_2–C_4 dicarboxylic acids in the marine aerosols, Geophys. Res. Lett., 30, 1672, doi:10.1029/2003GL017451, 2003b.

Mochida, M., Umemoto, N., Kawamura, K., Lim, H. J., and Turpin, B. J.: Bimodal size distributions of various organic acids and fatty acids in the marine atmosphere: influence of anthropogenic aerosols, Asian dusts, and sea spray off the coast of East Asia, J. Geophys. Res., 112, D15209, doi:10.1029/2006JD007773, 2007.

Myriokefalitakis, S., Tsigaridis, K., Mihalopoulos, N., Sciare, J., Nenes, A., Kawamura, K., Segers, A., and Kanakidou, M.: In-cloud oxalate formation in the global troposphere: a 3-D modeling study, Atmos. Chem. Phys., 11, 5761–5782, doi:10.5194/acp-11-5761-2011, 2011.

Nenes, A., Pandis, S. N., and Pilinis, C.: ISORROPIA: a new thermodynamic equilibrium model for multiphase multicomponent inorganic aerosols, Aquat. Geochem., 4, 123–152, 1998.

Pakkanen, T. A., Loukkola, K., Korhonen, C. H., Aurela, M., Makela, T., Hillamo, R. E., Aarnio, P., Koskentalo, T., Kousa, A., and Maenhaut, W.: Sources and chemical composition of atmospheric fine and coarse particles in the Helsinki area, Atmos. Environ., 35, 5381–5391, 2001.

Pope, C. A. and Dockery, D. W.: Health effects of fine particulate air pollution: lines that connect, J. Air Waste Manage., 56, 709–742, 2006.

Pradeep Kumar, P., Broekhuizen, K., and Abbatt, J. P. D.: Organic acids as cloud condensation nuclei: Laboratory studies of highly soluble and insoluble species, Atmos. Chem. Phys., 3, 509–520, doi:10.5194/acp-3-509-2003, 2003.

Quinn, P. K., Covert, D. S., Bates, T. S., Kapustin, V. N., Ramseybell, D. C., and Mcinnes, L. M.: Dimethylsulfide cloud condensation nuclei climate system–relevant size-resolved measurements of the chemical and physical-properties of atmospheric aerosol-particles, J. Geophys. Res., 98, 10411–10427, 1993.

Ramanathan, V., Crutzen, P. J., Kiehl, J. T., and Rosenfeld, D.: Atmosphere – aerosols, climate, and the hydrological cycle, Science, 294, 2119–2124, 2001.

Diacids and related compounds in spring aerosols from Okinawa Island

D. K. Deshmukh et al.

Title Page

Abstract	Introduction
Conclusions	References
Tables	Figures

◄ | ►►

◄ | ►

Back | Close

Full Screen / Esc

Printer-friendly Version

Interactive Discussion

Seinfeld, J. H. and Pandis, S. N.: Atmospheric Chemistry and Physics, John Wiley & Sons, New York, 1998.

Seinfeld, J. H. and Pandis, S. N.: Atmospheric Chemistry and Physics: From Air Pollution to Climate Change, 2nd edn., J. Wiley, New York, 2006.

Seinfeld, J. H. and Pankow, J. F.: Organic atmospheric particulate material, Annu. Rev. Phys. Chem., 54, 121–140, 2003.

Sempéré, R. and Kawamura, K.: Trans-hemispheric contribution of C_2–C_{10} α,ω-dicarboxylic acids, and related polar compounds to water-soluble organic carbon in the western Pacific aerosols in relation to photochemical oxidation reactions, Global Biogeochem. Cy., 17, 1069, doi:10.1029/2002GB001980, 2003.

Takami, A., Miyoshi, T., Shimono, A., Kaneyasu, N., Kato, S., Kajii, Y., and Hatakeyama, S.: Transport of anthropogenic aerosols from Asia and subsequent chemical transformation, J. Geophys. Res., 112, D22S31, doi:10.1029/2006jd008120, 2007.

Takiguchi, Y., Takami, A., Sadanaga, Y., Lun, X. X., Shimizu, A., Matsui, I., Sugimoto, N., Wang, W., Bandow, H., and Hatakeyama, S.: Transport and transformation of total reactive nitrogen over the East China Sea, J. Geophys. Res., 113, D10306, doi:10.1029/2007jd009462, 2008.

Tao, J., Zhang, L., Engling, G., Zhang, R., Yang, T., Cao, J., Zhu, C., Wang, Q., and Luo, L.: Chemical composition of $PM_{2.5}$ in an urban environment in Chengdu, China: importance of springtime dust storms and biomass burning, Atmos. Res., 122, 270–283, 2013.

Tao, S., Wang, Y., Wu, S. M., Liu, S. Z., Dou, H., Liu, Y. N., Lang, C., Hu, F., and Xing, B. S.: Vertical distribution of polycyclic aromatic hydrocarbons in atmospheric boundary layer of Beijing in winter, Atmos. Environ., 41, 9594–9602, 2007.

Tsai, Y. I. and Chen, C. L.: Characterization of Asian dust storm and non-Asian dust storm $PM_{2.5}$ aerosol in southern Taiwan, Atmos. Environ., 40, 4734–4750, 2006.

Turpin, B. J. and Lim, H. J.: Species contributions to $PM_{2.5}$ mass concentrations: revisiting common assumptions for estimating organic mass, Aerosol. Sci. Tech., 35, 602–610, 2001.

Volkamer, R., Platt, U., and Wirtz, K.: Primary and secondary glyoxal formation from aromatics: experimental evidence for the bicycloalkyl-radical pathway from benzene, toluene, and *p*-xylene, J. Phys. Chem. A, 105, 7865–7874, 2001.

Wang, G. H., Kawamura, K., Xie, M. J., Hu, S. Y., Li, J. J., Zhou, B. H., Cao, J. J., and An, Z. S.: Selected water-soluble organic compounds found in size-resolved aerosols collected from urban, mountain and marine atmospheres over East Asia, Tellus, 63, 371–381, 2011.

Diacids and related compounds in spring aerosols from Okinawa Island

D. K. Deshmukh et al.

Title Page

Abstract	Introduction
Conclusions	References
Tables	Figures

|◄ | ►|

◄ | ►

Back | Close

Full Screen / Esc

Printer-friendly Version

Interactive Discussion

Wang, G. H., Kawamura, K., Cheng, C. L., Li, J. J., Cao, J. J., Zhang, R. J., Zhang, T., Liu, S. X., and Zhao, Z. Z.: Molecular distribution and stable carbon isotopic composition of dicarboxylic acids, ketocarboxylic acids, and alpha-dicarbonyls in size-resolved atmospheric particles from Xi'an city, China, Environ. Sci. Technol., 46, 4783–4791, 2012.

Wang, G. H., Zhou, B. H., Cheng, C. L., Cao, J. J., Li, J. J., Meng, J. J., Tao, J., Zhang, R. J., and Fu, P. Q.: Impact of Gobi desert dust on aerosol chemistry of Xi'an, inland China during spring 2009: differences in composition and size distribution between the urban ground surface and the mountain atmosphere, Atmos. Chem. Phys., 13, 819–835, doi:10.5194/acp-13-819-2013, 2013.

Wang, H., Kawamura, K., and Shooter, D.: Carbonaceous and ionic components in wintertime atmospheic aeosols from two New Zwaland cities: implication for solid fuel combustion, Atmos. Environ., 39, 5865–5875, 2005a.

Wang, Y., Zhuang, G. S., Sun, Y., and An, Z. S.: Water-soluble part of the aerosol in the dust storm season – evidence of the mixing between mineral and pollution aerosols, Atmos. Environ., 39, 7020–7029, 2005.

Warneck, P.: In-cloud chemistry opens pathway to the formation of oxalic acid in the marine atmosphere, Atmos. Environ., 37, 2423–2427, 2003.

Yamasoe, M. A., Artaxo, P., Miguel, A. H., and Allen, A. G.: Chemical composition of aerosol particles from direct emissions of vegetation fires in the Amazon Basin: water-soluble species and trace elements, Atmos. Environ., 34, 1641–1653, 2000.

Yao, X. H., Fang, M., and Chan, C. K.: Size distributions and formation of dicarboxylic acids in atmospheric particles, Atmos. Environ., 36, 2099–2107, 2002.

Zimmermann, J. and Poppe, D.: A supplement for the RADM2 chemical mechanism: the photooxidation of isoprene, Atmos. Environ., 30, 1255–1269, 1996.

Title Page

Abstract   Introduction

Conclusions   References

Tables   Figures

◀◀   ▶▶

◀   ▶

Back   Close

Full Screen / Esc

Printer-friendly Version

Interactive Discussion

Table 1. Concentrations ($\mu g\,m^{-3}$) of carbonaceous species and major inorganic ions in the fine and coarse mode aerosols in Okinawa Island in the Western North Pacific.

Inorganic ions	Fine mode[a]				Coarse mode[b]			
	Mean	S.D.[c]	Min.[d]	Max.[e]	Mean	S.D.	Min.	Max.
Water-soluble inorganic ions								
Cations								
Na^+	0.44	0.20	0.21	0.72	2.42	0.89	1.60	3.65
NH_4^+	2.40	1.18	0.74	3.69	0.03	0.01	0.03	0.05
K^+	0.14	0.06	0.04	0.21	0.09	0.02	0.07	0.12
Mg^{2+}	0.07	0.02	0.04	0.10	0.34	0.11	0.24	0.49
Ca^{2+}	0.06	0.02	0.04	0.09	0.41	0.19	0.15	0.60
Total cations	3.12	1.22	1.28	4.37	3.29	1.02	2.55	4.82
Anions								
MSA^-	0.04	0.01	0.03	0.06	0.01	0.00	0.00	0.01
Cl^-	0.12	0.13	0.02	0.29	4.27	2.25	1.77	7.25
NO_3^-	0.14	0.08	0.04	0.23	1.61	0.54	0.94	2.41
SO_4^{2-}	10.1	4.85	2.88	14.9	1.46	0.44	0.69	1.81
Total anions	10.4	4.73	3.33	15.1	7.35	2.20	5.69	10.6
Total water-soluble ions								
Total water-soluble ions	13.5	5.95	4.61	19.5	10.6	3.22	8.33	15.4
Carbonaceous components								
WSOC	1.12	0.49	0.31	1.61	0.33	0.13	0.15	0.52
OC	1.62	0.59	0.62	2.12	0.60	0.17	0.36	0.82
EC	0.05	0.03	0.00	0.09	–	–	–	–
TC	1.67	0.65	0.62	2.41	0.60	0.17	0.36	0.82

[a] Fine mode represents aerosol size of $D_p < 2.1\,\mu m$.

[b] Coarse mode represents aerosol size of $D_p > 2.1\,\mu m$.

[c] Standard deviation.
[d] Minimum.
[e] Maximum.

Table 2. Concentrations ($ng\,m^{-3}$) of water-soluble dicarboxylic acids and related polar compounds in the fine and coarse mode aerosols in Okinawa Island in the Western North Pacific.

Compounds	Abbreviation	Chemical formula	Fine mode[a] Mean	S.D.[c]	Min.[d]	Max.[e]	Coarse mode[b] Mean	S.D.	Min.	Max.
			Dicarboxylic acids							
Saturated normal-chain diacids										
Oxalic	C_2	HOOC–COOH	135	37.4	76.0	176	40.2	14.7	22.1	60.0
Malonic	C_3	HOOC–CH$_2$–COOH	19.5	6.84	7.56	23.6	12.4	3.52	6.87	15.5
Succinic	C_4	HOOC–(CH$_2$)$_2$–COOH	13.4	4.98	5.08	17.5	8.02	2.21	4.66	10.1
Glutaric	C_5	HOOC–(CH$_2$)$_3$–COOH	3.30	1.54	1.00	4.75	1.89	0.57	1.07	2.66
Adipic	C_6	HOOC–(CH$_2$)$_4$–COOH	3.49	1.09	2.47	4.98	2.50	1.24	1.45	4.23
Pimelic	C_7	HOOC–(CH$_2$)$_5$–COOH	0.46	0.24	0.04	0.63	0.32	0.11	0.20	0.44
Suberic	C_8	HOOC–(CH$_2$)$_6$–COOH	0.07	0.07	0.00	0.16	0.04	0.02	0.02	0.07
Azelaic	C_9	HOOC–(CH$_2$)$_7$–COOH	1.20	0.72	0.51	2.41	1.15	0.60	0.49	2.10
Decanedioic	C_{10}	HOOC–(CH$_2$)$_8$–COOH	0.17	0.11	0.01	0.30	0.08	0.07	0.03	0.19
Undecanedioic	C_{11}	HOOC–(CH$_2$)$_9$–COOH	0.47	0.33	0.13	0.76	0.25	0.10	0.14	0.38
Dodecanedioic	C_{12}	HOOC–(CH$_2$)$_{10}$–COOH	0.07	0.03	0.03	0.09	0.05	0.02	0.02	0.07
Branched-chain diacids										
Methylmalonic	iC$_4$	HOOC–CH(CH$_3$)–COOH	0.43	0.23	0.09	0.71	0.47	0.37	0.09	0.99
Methylsuccinic	iC$_5$	HOOC–CH(CH$_3$)–COOH	0.81	0.27	0.37	1.00	0.59	0.13	0.45	0.80
2-Methylglutaric	iC$_6$	HOOC–CH(CH$_3$)–(CH$_2$)$_2$–COOH	0.35	0.24	0.05	0.70	0.19	0.20	0.04	0.53
Unsaturated aliphatic diacids										
Maleic	M	HOOC–CH=CH–COOH - cis	0.81	0.25	0.41	1.05	0.73	0.23	0.37	0.95
Fumaric	F	HOOC–CH=CH–COOH - trans	0.31	0.09	0.20	0.42	0.21	0.08	0.12	0.30
Methylmaleic	mM	HOOC–C(CH$_3$) =CH–COOH - cis	0.34	0.27	0.11	0.76	0.57	0.48	0.11	1.37
Unsaturated aromatic diacids										
Phthalic	Ph	HOOC–(C$_6$H$_4$)–COOH - o-isomer	6.29	2.85	1.99	9.3	2.79	0.81	1.85	3.9
Isophthalic	iPh	HOOC–(C$_6$H$_4$)–COOH - m-isomer	0.46	0.07	0.35	0.55	0.17	0.06	0.09	0.22
Terephthalic	tPh	HOOC–(C$_6$H$_4$)–COOH - p-isomer	2.21	1.15	0.32	3.30	0.64	0.38	0.09	1.17
Multifunctional diacids										
Malic	hC$_4$	HOOC–CH(OH)–CH$_2$–COOH	0.14	0.05	0.11	0.21	0.14	0.06	0.07	0.20
Ketomalonic	kC$_3$	HOOC–HC(O)–COOH	4.92	3.79	0.46	9.28	0.49	0.17	0.32	0.77
4-Ketopimelic	kC$_7$	HOOC–CH$_2$–CH$_2$–HC(O) (CH$_2$)$_2$–COOH	2.57	0.83	1.26	3.20	0.43	0.16	0.26	0.69
Total diacids			196	58.1	98.3	253	74.1	24.3	41.4	105
			ω -Oxocarboxylic acids							
Glyoxylic	ωC$_2$	OHC–COOH	14.1	5.92	4.77	20.2	4.81	2.00	2.23	7.20
3-Oxopropanoic	ωC$_3$	OHC–CH$_2$–COOH	0.08	0.05	0.00	0.12	0.05	0.04	0.02	0.12
4-Oxobutanoic	ωC$_4$	OHC–(CH$_2$)$_2$–COOH	2.23	1.12	0.86	3.56	0.68	0.35	0.41	1.22
9-Oxononanoic	ωC$_9$	OHC–(CH$_2$)$_7$–COOH	0.74	0.20	0.54	1.07	1.06	0.34	0.57	1.41
Total oxoacids			17.1	7.04	6.27	25.0	6.60	2.33	3.26	9.52
			Ketoacid							
Pyruvic	Pyr	CH$_3$–(O)C–COOH	2.61	0.76	1.67	3.48	2.32	1.20	0.76	4.09
			α–Dicarbonyls							
Glyoxal	Gly	OHC–CHO	2.74	1.12	1.45	4.40	0.84	0.26	0.50	1.17
Methylglyoxal	MeGly	CH$_3$–(O)C–CHO	1.09	0.98	0.25	2.53	0.65	0.16	0.45	0.87
Total α-dicarbonyls			2.83	1.59	1.03	4.68	1.49	0.37	0.96	1.86
			Aromatic monoacid							
Benzoic acid		H$_5$C$_6$–COOH	16.5	11.0	4.57	28.3	1.98	1.01	0.70	3.38

[a] Fine mode represents aerosol size of $D_p < 2.1\,\mu m$.
[b] Coarse mode represents aerosol size of $D_p > 2.1\,\mu m$.
[c] Standard deviation.
[d] Minimum.
[e] Maximum.

Table 3. Pearson correlation coefficients[a] (r) matrix among the selected measured chemical species/components in the fine and coarse mode aerosols in Okinawa Island in the Western North Pacific Rim.

Fine mode[b]

	Na^+	NH_4^+	K^+	Mg^{2+}	Ca^{2+}	MSA^-	Cl^-	NO_3^-	SO_4^{2-}	WSOC	OC	C_2	C_3	C_4	C_5	ωC_2	Pyr	Gly	MeGly	LWC
Na^+	1.00																			
NH_4^+	−0.25	1.00																		
K^+	−0.32	0.99	1.00																	
Mg^{2+}	0.98	−0.16	−0.23	1.00																
Ca^{2+}	−0.21	0.62	0.33	−0.15	1.00															
MSA^-	−0.32	0.92	0.92	−0.17	0.53	1.00														
Cl^-	0.65	−0.85	−0.85	0.58	−0.33	−0.78	1.00													
NO_3^-	0.65	−0.56	−0.55	0.68	0.22	−0.36	0.76	1.00												
SO_4^{2-}	−0.10	0.99	0.98	−0.02	0.59	0.89	−0.78	−0.49	1.00											
WSOC	0.10	0.91	0.93	0.16	0.30	0.79	−0.57	−0.27	0.96	1.00										
OC	0.12	0.91	0.95	0.16	0.25	0.80	−0.57	−0.32	0.93	0.96	1.00									
C_2	0.12	0.89	0.85	−0.13	0.22	0.80	−0.53	−0.30	0.92	0.99	0.98	1.00								
C_3	−0.05	0.90	0.89	−0.05	0.20	0.66	−0.68	−0.53	0.90	0.93	0.96	0.89	1.00							
C_4	−0.12	0.96	0.95	−0.09	0.15	0.76	−0.75	−0.55	0.96	0.95	0.96	0.92	0.99	1.00						
C_5	−0.12	0.99	0.96	−0.05	0.33	0.87	−0.80	−0.53	0.99	0.93	0.93	0.91	0.95	0.97	1.00					
ωC_2	0.11	0.92	0.90	0.19	0.19	0.82	−0.57	−0.25	0.96	0.99	0.99	0.99	0.90	0.93	0.95	1.00				
Pyr	0.01	0.93	0.88	0.12	0.39	0.88	−0.73	−0.33	0.96	0.88	0.87	0.85	0.80	0.86	0.96	0.91	1.00			
Gly	0.01	0.86	0.86	0.15	0.09	0.92	−0.52	−0.07	0.86	0.89	0.82	0.93	0.70	0.78	0.85	0.92	0.85	1.00		
MeGly	0.15	0.35	0.39	0.26	0.13	0.52	0.06	0.50	0.36	0.53	0.35	0.62	0.25	0.31	0.31	0.55	0.29	0.75	1.00	
LWC	0.16	0.87	0.83	0.30	0.53	0.88	−0.53	−0.13	0.92	0.90	0.87	0.92	0.82	0.83	0.89	0.95	0.95	0.95	0.55	1.00

Coarse mode[c]

	Na^+	NH_4^+	K^+	Mg^{2+}	Ca^{2+}	MSA^-	Cl^-	NO_3^-	SO_4^{2-}	WSOC	OC	C_2	C_3	C_4	C_5	ωC_2	Pyr	Gly	MeGly	LWC
Na^+	1.00																			
NH_4^+	0.60	1.00																		
K^+	0.96	0.77	1.00																	
Mg^{2+}	0.98	0.63	0.33	1.00																
Ca^{2+}	−0.12	0.03	−0.06	−0.29	1.00															
MSA^-	−0.15	−0.66	−0.03	−0.25	−0.02	1.00														
Cl^-	0.98	0.59	0.90	0.98	−0.27	−0.22	1.00													
NO_3^-	−0.30	−0.23	−0.15	−0.39	0.98	0.28	−0.55	1.00												
SO_4^{2-}	0.33	0.32	0.56	0.28	0.63	0.25	0.16	0.67	1.00											
WSOC	−0.18	−0.26	0.06	−0.20	0.23	0.55	−0.36	0.92	0.72	1.00										
OC	−0.11	−0.10	0.13	−0.10	0.21	0.36	−0.28	0.92	0.72	0.97	1.00									
C_2	−0.05	0.26	0.30	0.15	0.63	0.09	−0.08	0.88	0.76	0.93	0.82	1.00								
C_3	0.32	0.33	0.53	0.31	0.68	0.18	0.15	0.75	0.92	0.88	0.82	0.93	1.00							
C_4	0.33	0.39	0.60	0.35	0.53	0.16	0.33	0.32	0.88	0.31	0.55	0.36	0.63	1.00						
C_5	0.05	0.05	0.22	−0.06	0.62	0.32	−0.05	0.43	0.75	0.38	0.22	0.45	0.91		1.00					
ωC_2	0.23	0.37	0.85	0.68	0.12	0.42	0.59	0.23	0.73	0.53	0.52	0.53	0.76	0.60	0.32	1.00				
Pyr	−0.09	−0.01	0.13	−0.08	0.81	0.23	−0.26	0.93	0.73	0.99	0.93	0.96	0.90	0.33	0.28	0.49	1.00			
Gly	0.26	0.26	0.78	0.57	0.05	0.52	0.58	0.06	0.69	0.28	0.33	0.22	0.55	0.76	0.57	0.89	0.21	1.00		
MeGly	0.55	0.69	0.67	0.58	0.48	−0.20	0.48	0.18	0.77	0.16	0.13	0.25	0.58	0.93	0.75	0.49	0.22	0.59	1.00	
LWC	0.61	0.03	0.53	0.56	−0.70	0.48	0.63	−0.51	−0.10	−0.19	−0.13	−0.29	−0.08	−0.03	−0.22	0.57	−0.28	0.63	−0.13	1.00

See Table 1 and 2 for abbreviation.
[a] Correlation is significant at 0.05 level for the values where r is > 0.80.
[b] Fine mode represents aerosol size of D_p < 2.1 μm.
[c] Coarse mode represents aerosol size of D_p > 2.1 μm.

Title Page

Abstract | Introduction

Conclusions | References

Tables | Figures

|◄ | ►|

◄ | ►

Back | Close

Full Screen / Esc

Printer-friendly Version

Interactive Discussion
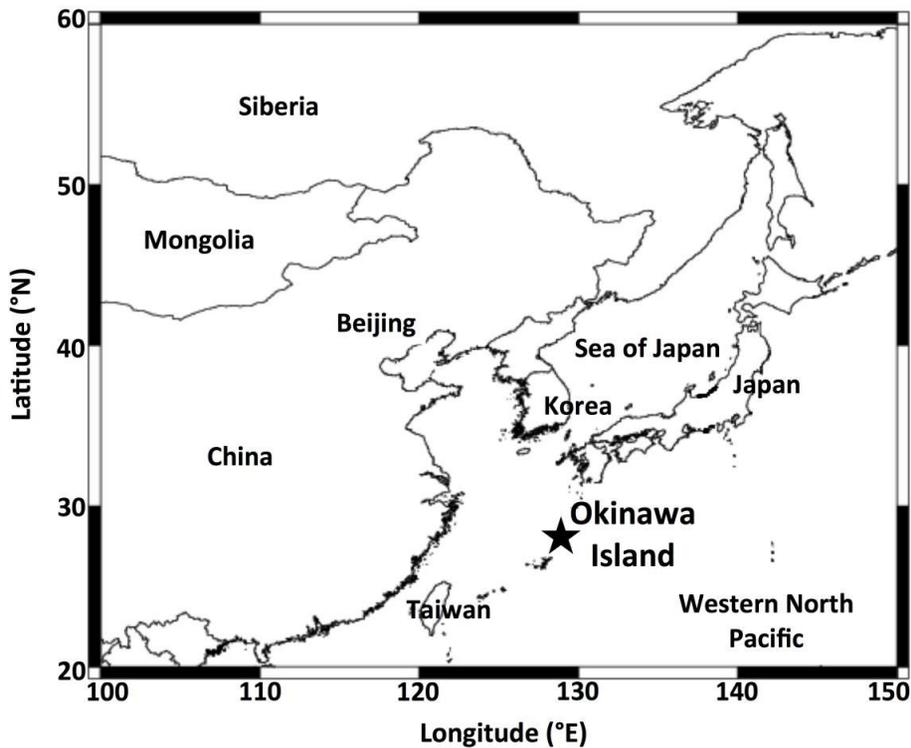
**Figure 1.** A map of East Asia with the location of Okinawa Island (26.87° N and 128.25° E) and major megacities in Asia.
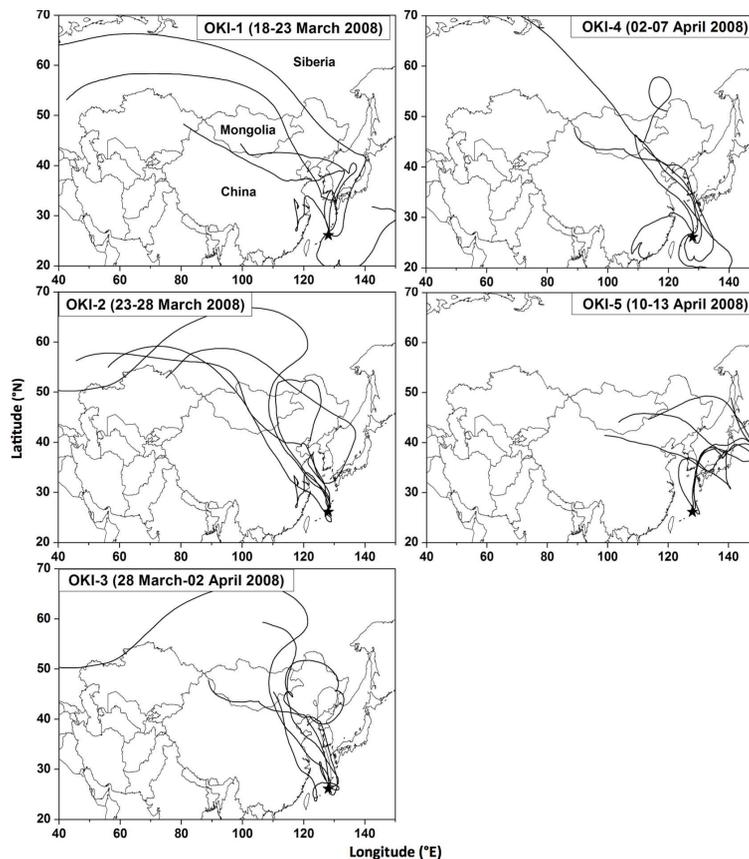
Figure 2. NOAA HYSPLIT seven-day backward air mass trajectories at 500 m a.g.l. for the aerosol samples at Okinawa Island.
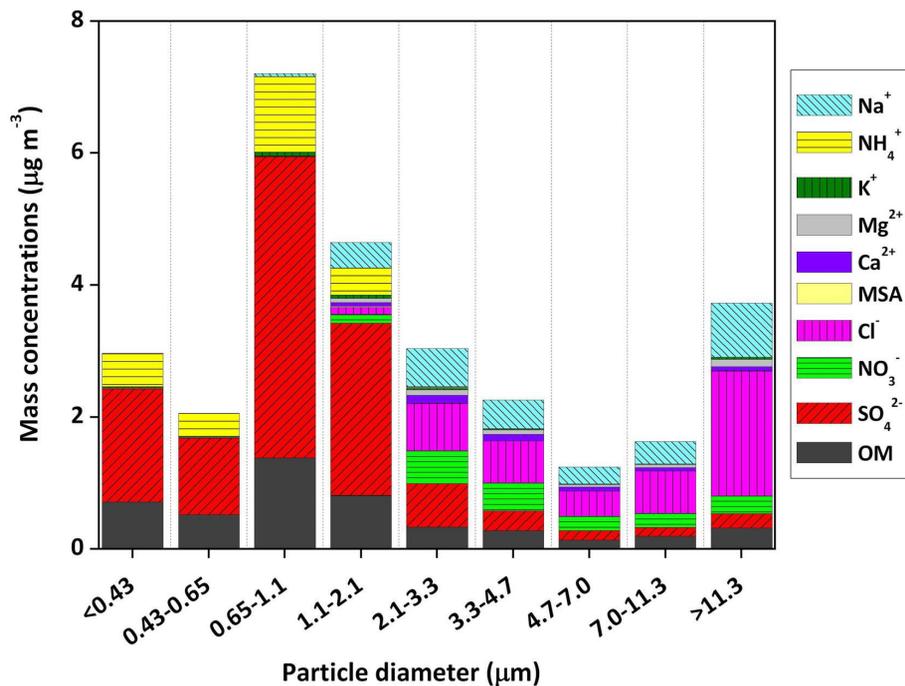
Figure 3. Average size-segregated chemical composition of spring aerosols collected at Okinawa Island.
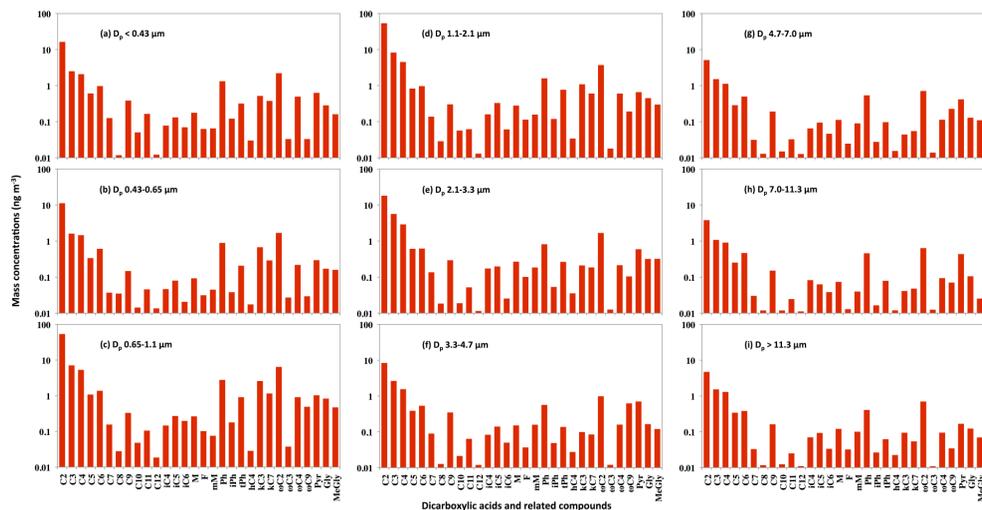
Figure 4. Average molecular distributions of water-soluble dicarboxylic acids and related compounds in size-segregated aerosols collected at Okinawa Island.
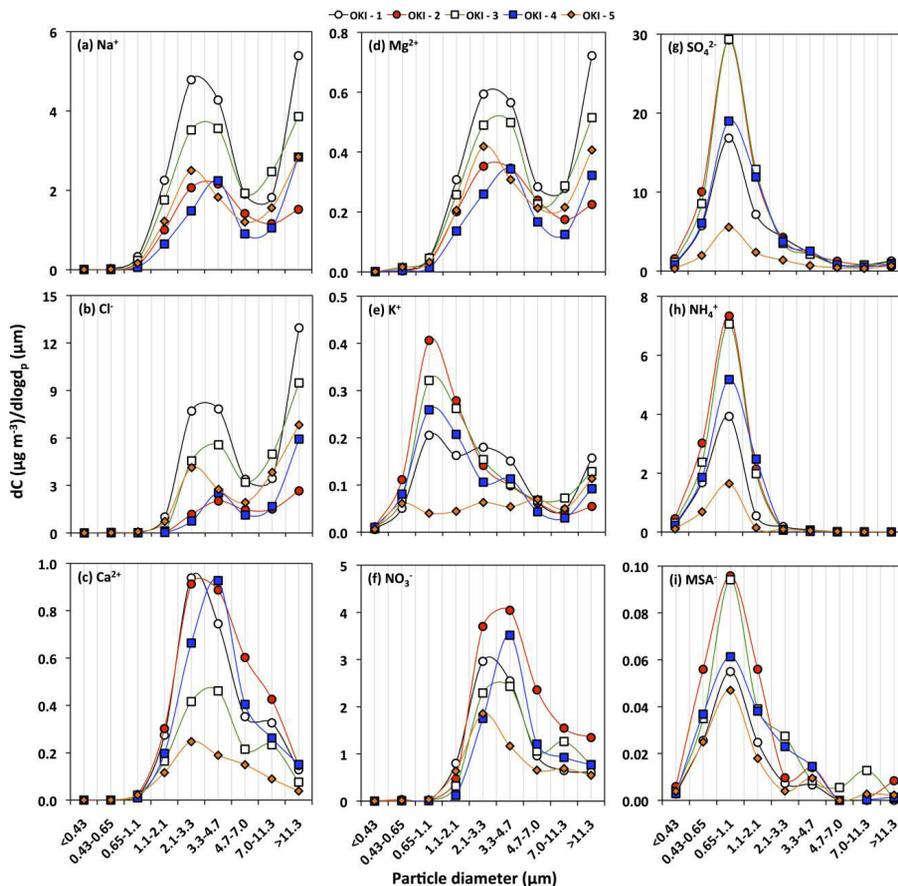
Figure 5. Size distributions of water-soluble inorganic ions in the aerosol samples collected at Okinawa Island.

ACPD

15, 26509–26554, 2015

Diacids and related compounds in spring aerosols from Okinawa Island

D. K. Deshmukh et al.

Title Page

Abstract | Introduction

Conclusions | References

Tables | Figures

|◄ | ►|

◄ | ►

Back | Close

Full Screen / Esc

Printer-friendly Version

Interactive Discussion
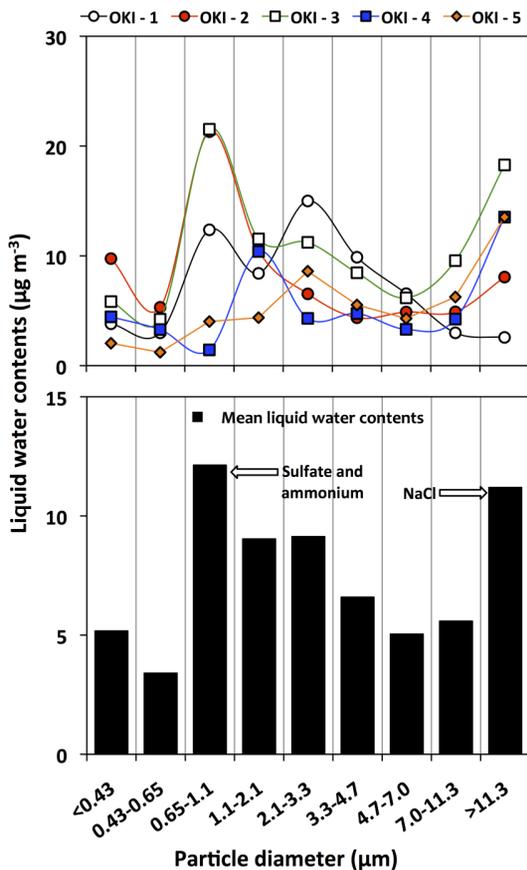
Figure 6. Aerosol liquid water contents for each sample in size-segregated aerosols and mean liquid water contents of size-segregated aerosols at Okinawa Island.
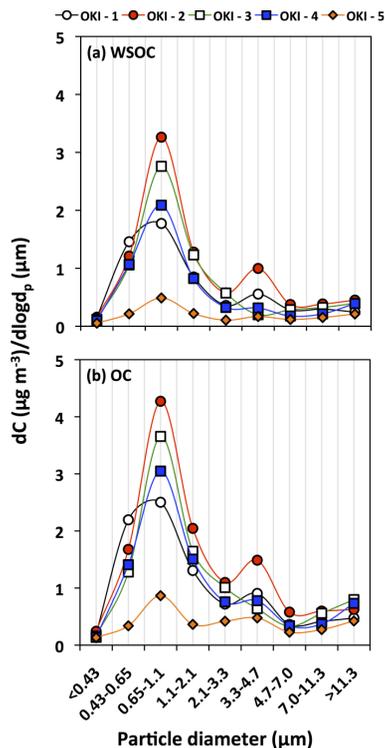
Figure 7. Size distributions of water-soluble organic carbon (WSOC) and organic carbon (OC) in the aerosol samples collected at Okinawa Island.
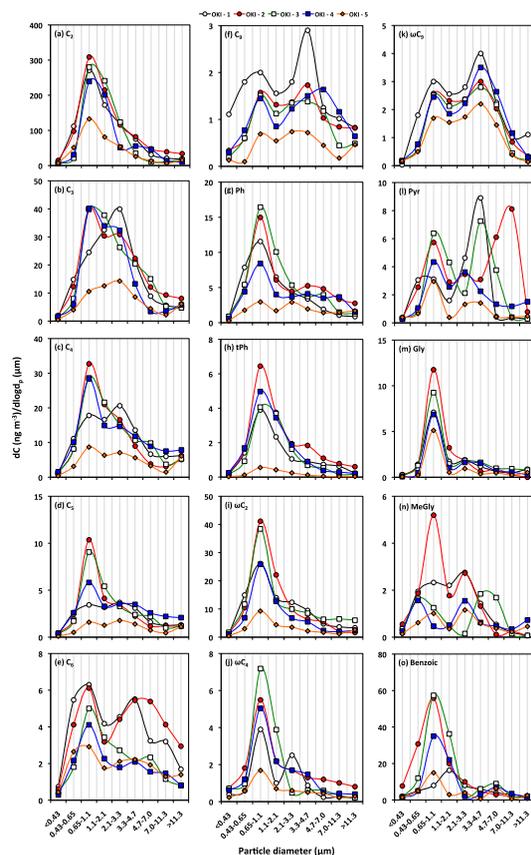
Figure 8. Size distributions of selected water-soluble dicarboxylic acids and related compounds in the aerosol samples collected at Okinawa Island.
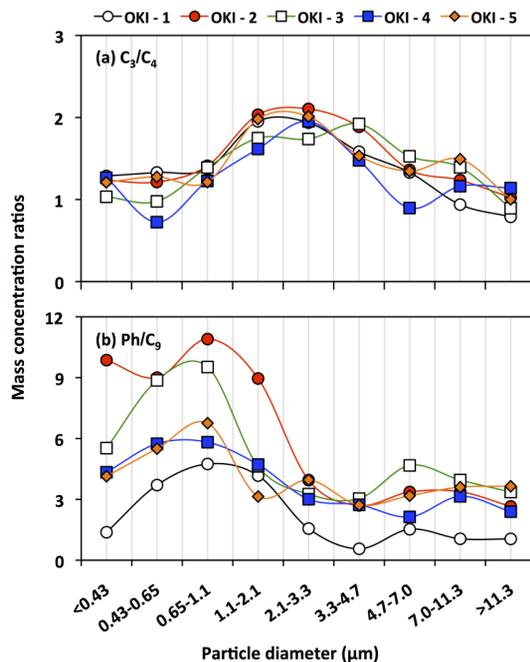
Figure 9. Mass concentration ratio of malonic to succinic acid and phthalic to azelaic acid in size-segregated aerosols collected at Okinawa Island.